International Journal of Biological Macromolecules 306 (2025) 141499

Contents lists available at ScienceDirect

International Journal of Biological Macromolecules

journal homepage: www.elsevier.com/locate/ijbiomac

Anticoagulant potential of sulfated galactofucan from *Turbinaria ornata*: Targeting coagulation pathways and thrombin signaling in human umbilical vein endothelial cells

Ans Mariya George [a,b], Kajal Chakraborty [a,*], Silpa Kunnappilly Paulose [a], Shifa Jalal [a], Ashwin Ashok Pai [a,c], Shubhajit Dhara [a,c]

[a] ICAR-Central Marine Fisheries Research Institute, Ernakulam North P.O., P.B. No. 1603, Cochin, Kerala State, India
[b] Faculty of Marine Sciences, Lakeside Campus, Cochin University of Science and Technology, Cochin, Kerala State, India
[c] Department of Chemistry, Mangalore University, Mangalagangothri 574199, Karnataka State, India

ARTICLE INFO

Keywords:
Brown seaweed *Turbinaria ornata*
Sulfated polysaccharide
Thrombin-catalyzed fibrin polymerization

ABSTRACT

Dysregulation of blood coagulation can result in thrombosis, highlighting the importance of anticoagulants that target both the extrinsic and intrinsic pathways of fibrin clot formation. This study explores anticoagulant effects of TO_{SP}-3, a sulfated polysaccharide characterized as [→3)-4-*O*-SO_3-α-Fuc*p*-(1 → 3)-4-*O*-SO_3-β-Gal*p*-(1→] from the brown seaweed *Turbinaria ornata*, composed of sulfated α-(1 → 3)-fucopyranose (Fuc*p*) and β-(1 → 3)-galactopyranose (Gal*p*) units. In vitro analysis revealed that TO_{SP}-3 (25 μg/mL) markedly extended activated partial thromboplastin time (100.49 s) and prothrombin time (77.57 s), highlighting its regulation on both intrinsic and extrinsic coagulation cascades. TO_{SP}-3 induced a substantial reduction in coagulation factor Xa (FXa) expression (89 %) in human umbilical vein endothelial cells. It further exhibited a substantial five-fold inhibition of thrombin-catalyzed fibrin polymerization and reduced platelet aggregation by approximately 87 %, compared to the negative control (10 μM ADP). TO_{SP}-3 attenuated thrombin-induced intracellular Ca^{2+} mobilization (~33 %), while concurrently diminishing total thrombin production (33 %), thereby highlighting its inhibitory effects on thrombin-mediated signaling pathways. The sulfate content, structural patterns, and linkage characteristics of TO_{SP}-3 may enable it to inhibit FXa expression and suppress thrombin-catalyzed fibrin polymerization through electrostatic interactions, potentially offering more effective modulation of the coagulation cascade than heparin. These findings highlight the potential of TO_{SP}-3 as a natural anticoagulant for attenuating thrombotic disorders.

1. Introduction

Seaweeds are prolific sources of structurally diverse polyanionic polysaccharides, particularly sulfated polysaccharides (SPs), which exhibit significant potential for therapeutic applications and drug development [1]. Specifically, brown seaweeds are rich in acidic polysaccharides, such as fucoidan, and alginate, as well as sulfated fucans (homo/heterofucans), which feature complex branching patterns, varied sulfate distributions, and in some cases, the presence of acetyl moieties [2]. These polysaccharides possess significant pharmacological importance, attributed to their ability to interact with cellular components and functional proteins, positioning them as promising candidates for pharmaceutical applications [3]. Among these polysaccharides, sulfated fucans are particularly prominent and have been reported in various brown seaweed species, including *Cladosiphon okamuranus*, *Ecklonia cava*, *Undaria pinnatifida*, and *Ascophyllum nodosum* [4]. The structural diversity of these fucans has been categorized into two main types. Type I fucans consist of repeating units of α-L-fucopyranose connected through (1 → 3)-glycosidic bonds, while type II fucans are composed of α-L-fucopyranose units intricately linked by alternating (1 → 3) and (1 → 4) glycosidic bonds [5,6]. Additionally, brown seaweeds like *Adenocystis utricularis* produce unique variants like galactofucans, which are rich in D-galactose, L-fucose, and ester sulfate groups, and uronofucoidans, characterized by fucose alongside diverse monosaccharides, and substantial amounts of uronic acids [7]. This diversity in sulfated fucans accentuates the complexity and functional

* Corresponding author at: Marine Biotechnology Fish Nutrition and Health Division, ICAR-Central Marine Fisheries Research Institute, Ernakulam North P.O., P.B. No. 1603, Cochin, India.
E-mail address: kajal_cmfri@yahoo.com (K. Chakraborty).

https://doi.org/10.1016/j.ijbiomac.2025.141499
Received 21 December 2024; Received in revised form 7 February 2025; Accepted 24 February 2025
Available online 25 February 2025

significance of polysaccharides derived from brown algae.

Thrombosis is the abnormal formation of blood clots within the vasculature, contributing to a significant global health challenge. Arterial thrombosis, in particular, often results from the rupture or instability of atherosclerotic plaques, triggering clot formation that obstructs blood flow and can lead to life-threatening events, such as heart attacks and strokes [8]. The coagulation cascade, fundamental to hemostasis, comprises multifaceted processes, primarily divided into two distinct but converging pathways. The intrinsic pathway is activated by endothelial disruption, leading to the activation of several coagulation proteins VIII, XII, IX, and XI. Conversely, the extrinsic pathway is initiated by tissue injury, wherein tissue factor (TF) interacts with and activates factor VII, triggering the activation of factor Xa [9]. Both pathways eventually converge at factor Xa, which, in conjunction with factor V and Ca^{2+} ions, facilitates the conversion of prothrombin to thrombin. Thrombin later converts fibrinogen into fibrin, forming a stable clot that effectively halts bleeding [10]. While this cascade is essential for preventing hemorrhage following injury, its dysregulation can lead to excessive clot formation, resulting in thrombotic events [11]. Anticoagulants mitigate thrombosis by disrupting the key steps in this cascade. Common anticoagulant therapies and direct oral anticoagulants function by inhibiting specific factors within this cascade, thereby reducing clot formation [12]. However, despite their targeted mechanisms of action within this intricate cascade, these therapies are prone to adverse side effects, such as bleeding complications and complex drug interactions. Furthermore, heparin, while effective, can paradoxically induce heparin-induced thrombocytopenia (HIT), complicating its therapeutic profile [13,14]. Consequently, there is a growing emphasis on developing safer and more effective anticoagulants derived from natural sources. Among these, brown seaweeds, have emerged as promising candidates. Sulfated polysaccharides derived from these seaweeds have demonstrated anticoagulant activity by targeting various steps in the coagulation cascade, offering potential as therapeutic agents that may reduce clot formation without the adverse bleeding risks associated with conventional anticoagulants [15,16].

Previous studies have reported that sulfated fucans from seaweeds belonging to the Phaeophyceae class, including *Laminaria japonica* and *Turbinaria decurrens*, exhibit significant anticoagulant and antithrombotic properties [17,18]. The anticoagulant efficacy of sulfated fucans is intricately linked to their structural features as branched variants inhibiting thrombin, while the linear forms activate antithrombin, and 4-*O*-sulfated fucose units demonstrate notable anticoagulant properties [19]. Further, specific sulfation patterns and glycosidic linkages contribute to their anticoagulant potency, emphasizing the structure-dependent nature of this bioactivity [20]. Previous studies have demonstrated that sulfated fucans potentiate antithrombin III activity, thereby inhibiting both thrombin and factor Xa, key enzymes in the coagulation pathway, effectively preventing clot formation [21]. In addition, these polysaccharides activate heparin cofactor II, resulting in further thrombin inhibition, while also reducing platelet aggregation, which diminishes the risk of thrombosis [22]. This multifaceted mechanism positions sulfated polysaccharides as potent natural anticoagulants with modes of action comparable to those of heparin.

Brown seaweeds of the genus *Turbinaria* are widely distributed across marine ecosystems and are known for their high content of sulfated polysaccharides, which can constitute up to 45 % of their dry weight, with fucoidan comprising approximately 23 % of this total [23]. Among them, *Turbinaria ornata* (Family: Sargassaceae) is abundant in tropical and subtropical waters of the Pacific and Indian Oceans. Sulfated polysaccharides from brown seaweeds, particularly fucoidan, have been widely studied for their biological activities, including anticoagulant properties [19]. However, research on the anticoagulant potential of sulfated polysaccharides from *T. ornata* remains limited, particularly regarding their mechanism of action and the role of structural attributes on bioactivity. Based on these facts, the present study aims to isolate and characterize a sulfated polysaccharide (TO_{SP}-3) from *T. ornata*, and to evaluate its anticoagulant potential by detailed in vitro cell models. In order to accomplish these objectives, the putative structural formula of TO_{SP}-3 was elucidated using comprehensive spectroscopic techniques, including Fourier transform infrared (FTIR) spectroscopy, one- and two-dimensional nuclear magnetic resonance (NMR), high-resolution electrospray ionization mass spectrometry {HR(ESI)MS}, and gas chromatography mass spectrometry (GC–MS). The anticoagulant effects of TO_{SP}-3 were evaluated by assessing its impact on prothrombin time (PT) along with activated partial thromboplastin time (aPTT), reflecting its effect on coagulation factors in the extrinsic and intrinsic coagulation pathways, respectively. Additionally, the study explored key anticoagulant mechanisms in human umbilical vein endothelial cells (HUVECs), including phospho-MARCKS expression, Factor Xa inhibition, thrombin-mediated fibrin polymerization, platelet aggregation, and thrombin-induced intracellular calcium mobilization, which collectively influence the coagulation cascade. Furthermore, to gain insights into the role of structural attributes in enhancing anticoagulant activity, a structure–activity relationship study was conducted by comparing the physicochemical and molecular parameters of TO_{SP}-3 with a hypothetical non-sulfated variant, examining the impact of sulfation on bioactivity. Collectively, these analyses aim to demonstrate the multifaceted anticoagulant properties of TO_{SP}-3, supporting its potential as a promising candidate for anticoagulant treatment.

2. Materials and methods

2.1. Reagents and instrumentation

HUVECs, aPTT reagent, PT reagent, Goat anti-Rabbit IgG (H + L) cross-adsorbed antibody (Alexa Fluor® 594), and Fluo-4 AM kit were procured from Thermo Fisher (Waltham, Massachusetts). Thrombin (factor II), heparin, and human ELISA Kit were obtained from Sigma-Aldrich (St. Louis, Missouri, U.S). Additional details on reagents and equipment are included in the Supplementary Material S1.

2.2. Seaweed harvesting and preprocessing

Fresh seaweed samples of *T. ornata* (Turner) J. Agardh, 1848, (voucher specimen deposited in the Marine Biodiversity Museum, ICAR-Central Marine Fisheries Research Institute, India, CMFRI Herbarium, 2018, Accession no. AB.3.1.2.3) was harvested from the Mandapam islands of Mannar Bay, in the Coromandel Coast (8°48′ N, 78°9′ E and 9°14′ N, 79°14′ E), India. Approximately 10 kg of biomass was harvested, and species identification was confirmed through morphological traits and comparison with authenticated CMFRI herbarium specimens (Accession no. AB.3.1.2.3). The specimens were hand-harvested and thoroughly washed with water to remove impurities. Individual thalli were then placed in individual zip-lock bags and transported to research lab, where they were air-dried in the shade up to 3–5 days at ambient conditions. Once dried, the seaweed was pulverized into powder and preserved in airtight containers for future analysis.

2.3. Extraction of sulfated polysaccharide from the seaweed biomass

The pulverized seaweed (~100 g) was subjected to depigmentation with n-hexane (3500 mL, 60 °C) and then filtered to obtain the depigmented seaweed. The air-dried depigmented seaweed (100 g) was extracted twice using distilled water (1:20 *w*/v) at 80–85 °C for 4 h and then clarified by centrifugation (4000 ×*g*, 4 °C, 15 min, Thermo Scientific Sorvell ST 8R Centrifuge, MA). The supernatant (~3 L) was then reduced to one-tenth of its original volume (300 mL) using a vacuum concentrator system (Martin Christ RVC-2-33-IR; Germany), before being treated with 1 % (*w*/v) $CaCl_2$ and stored at 4 °C overnight to remove the alginate fraction (~14 *g*) by centrifugation (4600 ×*g*, 4 °C, 20 min). The supernatant (100 mL) was further precipitated with ice cold ethanol (~1.2 L; 1:4) and kept for 12 h at 4 °C. The resultant

precipitate was recovered by centrifugation (4600 ×*g*, 4 °C, 20 min) and lyophilized to yield the crude polysaccharide (TO_{SP}; 5.40 g) [24,25]. The percentage yield of TO_{SP} was evaluated using the formula:

$$\text{Yield of polysaccharide (\%)} = \frac{Weight of TOsp}{Weight of pulverized seaweed for aqueous extraction} \times 100$$

2.4. Fractionation and spectral analysis of sulfated galactofucan

The crude polysaccharide (TO_{SP}) was fractionated by using a weak positively charged anion exchange resin DEAE-cellulose on an open glass column (20 cm × 5 cm) [25]. The DEAE-cellulose slurry (~50 g) was prepared in distilled water and allowed to swell for 3 h before being packed into the column and stabilized. About 4 g of TO_{SP} was dissolved in 10 mL distilled water and then fractionated on a pre-packed column. The elution was initiated with water and increasing NaCl gradient (from 0.05 to 0.4 M) to obtain six fractions TO_{SP}-0 to TO_{SP}-5. The fractions were analyzed for total carbohydrate [26], uronic acid [27], and sulfate content [28] (Supplementary material S2). The TO_{SP}-3 (NaCl-0.2 M) fraction, with higher carbohydrate and sulfate contents was hydrolyzed using trifluoroacetic acid (CF_3CO_2H, 2 M, 100 °C for 6 h). Subsequently, the hydrolyzed sample was analyzed for monosaccharide composition using RP-HPLC with mobile phase composition of 30:70 water-acetonitrile (*v*/v) attached to SofTA 300 ELSD evaporative light scattering detector. Structural characterization was performed using comprehensive spectroscopic techniques, such as FT-IR, NMR, and HR (ESI)MS. The linkage pattern of glycosyl residues was elucidated through GC–MS analysis of partially *O*-methylated alditol acetate derivatives (PMAAs), obtained using sequence of derivatization steps involving methylation, reductive cleavage, and acetylation (Supplementary material S3).

2.5. Preliminary antioxidant activity

In vitro antioxidant activity of the TO_{SP}-3 fraction was assessed using 2,2-diphenyl-1-picrylhydrazyl (DPPH•) and 2,2′-azino-bis-(3-ethylbenzothiazoline-6-sulfonic acid) ($ABTS^+$) radical scavenging assays [29]. The results were presented as IC_{50} values, indicating the concentration required to achieve 50 % inhibition of radical activity. Detailed procedure is provided in Supplementary material S4.

2.6. Coagulation assays: activated partial thromboplastin time (aPTT) and prothrombin time (PT)

The anticoagulant activity of TO_{SP}-3 was assessed using activated partial thromboplastin time (aPTT) and prothrombin time (PT) clotting assays following previously described method [30]. Citrated normal human plasma (50 μL) was mixed with 50 μL of TO_{SP}-3 at concentrations of 6.25, 12.5, and 25 μg/mL, followed by a 5 min incubation at 37 °C. For the aPTT assay, 100 μL of pre-incubated aPTT reagent was added, and the mixture was activated for 10 min at 37 °C before measuring the clotting time. In parallel, the PT assay involved the addition of 100 μL of pre-incubated PT reagent, and the resulting clotting time was recorded in seconds, with heparin at 6.25 μg/mL serving as the standard control.

2.7. In vitro anticoagulant activities of TO_{SP}-3 in HUVECs

2.7.1. Cell culture

Human umbilical vein endothelial cells (HUVECs), derived from the umbilical cord, were sourced from Thermo Fisher Scientific, USA (Cat. No: C0035C) and cultured in endothelial cell growth medium enriched with LVES (large vessel endothelial supplement) and 1 % penicillin-streptomycin, following the manufacturer's protocol. The cells were maintained in a humidified incubator at 37 °C with 5 % CO_2 to ensure optimal growth conditions. HUVECs are widely used in anticoagulant studies due to their critical role in regulating coagulation, including the inhibition of thrombin-mediated fibrin polymerization, platelet aggregation, and thrombin-induced intracellular calcium mobilization. As endothelial cells lining blood vessels, they provide a relevant in vitro model to assess the effects of anticoagulants, such as Factor Xa inhibitors, and to investigate the potential anticoagulant activity. To maintain uniformity in cellular properties, all experiments were conducted using cells at passage 2.

2.7.2. Cellular viability studies using MTT assay

Cell viability of HUVECs treated with TO_{SP}-3 polysaccharide was evaluated using 3-(4,5-dimethylthiazolyl-2)-2,5-diphenyltetrazolium bromide (MTT) assay [31]. Briefly, 20,000 cells/well were seeded into a 96-well plate and incubated for 12 h before being exposed to varied concentrations of TO_{SP}-3 (6.25, 12.5, 25, 50, and 100 μg/mL) and incubated up to 72 h at 37 °C in a CO_2 atmosphere of 5 %. MTT substrate at final concentration of 0.5 mg/mL was added and incubated for 3 h to facilitate the formation of formazan crystals. The medium was gently discarded, and DMSO was added to dissolve the crystals. Absorbance was recorded at 570 nm with 630 nm as the reference using an ELISA plate reader. Heparin (20–60 μM) was used as the standard.

2.7.3. Evaluation of phospho-MARCKS and coagulation factor Xa expression: fluorescence microscopy

The anticoagulant effects of TO_{SP}-3 were evaluated by examining its influence on the expression of phosphorylated-MARCKS (p-MARCKS) and coagulation factor (FXa) in HUVECs [32]. For the p-MARCKS study, HUVECs were seeded with 20,000 cells per well and incubated for 1 day, followed by treatment with TO_{SP}-3 at concentrations of 6.25, 12.5, and 25 μg/mL for an additional 24 h. Untreated cells and heparin served as controls. Following treatment, the cells were permeabilized, exposed to a primary anti-p-MARCKS antibody, and stained with Alexa Fluor® 594 secondary antibody. Similarly, the assessment of factor Xa involved treating HUVEC with the same dosages of TO_{SP}-3 (6.25, 12.5, and 25 μg/mL), with untreated cells and heparin (6.25 μg/mL) serving as controls. Post-treatment, the cells were fixed, permeabilized, and incubated with a human anti-Factor X/Xa polyclonal antibody, followed by Goat anti-Rabbit IgG-Fluor® 594. Fluorescence microscopy was then employed for imaging for both the p-MARCKS and FXa, and the data were analyzed with ImageJ software.

2.7.4. Measurement of intracellular Ca^{2+} mobilization: fluorimetry method

The anticoagulant effects of TO_{SP}-3 on thrombin-induced intracellular Ca^{2+} mobilization in HUVECs were evaluated using colorimetric analysis. Initially, HUVECs at a density of 20,000 cells per well were seeded in 96-well plates and allowed to grow for 12–14 h at 37 °C with 5 % CO_2. Following the removal of the spent media and a subsequent wash

with D-PBS, cells were prepared for calcium measurement. A calcium-sensitive fluorescent dye was solubilized in an assay buffer of HEPES (20 mM) in Hanks' balanced salt solution (HBSS) and probenecid (2.5 mM). The cells were pre-incubated with thrombin at 37 °C for 30 min under 5 % CO_2 followed by a wash with PBS. The cells were subsequently treated with TO_{SP}-3 at varying concentrations (6.25, 12.5, and 25 μg/mL), along with a positive control (heparin, 6.25 μg/mL), and incubated for 30 min. The Ca^{2+}-binding dye was introduced to load the cells, and kept for 30 min at 37 °C. Intracellular Ca^{2+} levels were quantified using the Fluo-4 AM kit, and fluorescence was measured with a fluorescent plate reader.

2.7.5. Thrombin-catalyzed fibrin polymerization and total thrombin production

The in vitro anticoagulant effects of TO_{SP}-3 on thrombin-mediated fibrin polymerization were assessed using colorimetric analysis. Plasma samples were incubated with TO_{SP}-3 at appropriate dosages of 6.25, 12.5, and 25 μg/mL, along with a positive control (heparin), for 20 min at ambient temperature. Following this incubation, the samples underwent a 3-fold dilution in 50 mM tris-buffered saline (TBS, pH 7.4) prior to the addition of thrombin (0.5 U/mL) to initiate clot formation. Turbidity from fibrin polymerization was measured by absorbance at 350 nm every 20 s for 20 min using a plate reader, with the data presented as a curve.

To evaluate the impact of TO_{SP}-3 on thrombin production in HUVECs, enzyme-linked immunosorbent assay (ELISA) was carried out. HUVECs were seeded at 20,000 cells/well in 96-well plates and allowed to incubate for 24 h. Following the removal of the media, the cells were subjected to treatment with TO_{SP}-3 at concentrations of 6.25, 12.5, and 25 μg/mL, while untreated cells and those treated with heparin (6.25 μg/mL) were employed as controls. Following 24 h treatment, PBS was used to wash the cells, which were then lysed with a lysis buffer, and the thrombin levels within the lysates were quantified in accordance with the manufacturer's specifications.

2.7.6. Anti-platelet aggregation: spectrophotometry and scanning electron microscopy

Anti-platelet aggregation was assessed by spectrophotometric assay to examine the anticoagulant effects of TO_{SP}-3, followed by ultrastructural analysis using scanning electron microscopy (SEM). Blood was collected from mice and treated with acid citrate dextrose (ACD). After centrifugation (170 ×*g*, 7 min), platelet-rich plasma (PRP) was isolated, and platelets were reconstituted in Tyrode's buffer without calcium at 3×10^8 cells/mL concentration. For the aggregation assay, 50 μL of platelets were pre-incubated with different dosages of TO_{SP}-3 (6.25, 12.5, and 25 μg/mL) or aspirin (10 mM) at 37 °C for 15 min. The platelets were then stimulated with 10 μM adenosine diphosphate (ADP) and incubated for 5 min with continuous stirring. The degree of platelet aggregation was recorded spectrophotometrically at 600 nm, and platelet aggregation percentage was determined employing the formula:

$$\%\text{of platelet aggregation} = (\text{OD of test}/\text{OD of ADP}) \times 100$$

Platelet aggregates were also analyzed under SEM after fixing with glutaraldehyde and dehydrating in ethanol. SEM images were captured at 2000× magnification to study the ultrastructural details.

2.8. Structure-activity correlation analysis

The structure-activity relationship studies of TO_{SP}-3 utilized ADME works Model Builder (Fujitsu Kyushu Systems Limited, ver 7.10.0.0) to derive meaningful correlations between its physicochemical properties, especially focusing on descriptors of steric, electronic, and hydrophobic attributes. To study the effects of sulfate substitutions in modulating the biological activity of TO_{SP}-3, a hypothetical desulfated variant namely, TO_{SP}-3DS was used, providing insights into the influence of functional groups, particularly sulfates on bioactivity (Supplementary material S5).

2.9. Analysis of data

The results, presented as mean ± standard deviation, were derived from four independent experiments ($n = 4$) and was examined employing SPSS statistics software (SPSS Inc., CA). Analysis of variance (ANOVA) was performed, and Tukey's post hoc test was applied for comparisons when significant differences were identified. Statistical significance was set at $p < 0.05$.

3. Results and discussion

3.1. Anticoagulant properties of sulfated polysaccharides from brown seaweeds

Sulfated polysaccharides from brown seaweeds are recognized for their diverse biological properties, encompassing anticoagulant, antiviral, and anti-inflammatory effects, along with cell proliferation and adhesion [33]. While heparin remains a widely used therapeutic agent for the management of coagulation disorders, its association with adverse outcomes, most notably hemorrhagic complications and thrombocytopenia, emphasizes the need for safer anticoagulant alternatives with improved safety profiles. Within this context, sulfated polysaccharides emerge as promising candidates, particularly due to their capacity to inhibit critical coagulation proteins, including Factor Xa and thrombin [34]. Their anticoagulant potency is intricately modulated by specific structural attributes [19]. Numerous species of brown algae, including *Turbinaria decurrens, Ecklonia kurome*, and *Saccharina latissima*, have demonstrated both anticoagulant and antithrombotic potential in previous investigations [4,35].

3.2. Recovery yield and biochemical profile of TO_{SP}-3

Aqueous extraction of *T. ornata*, followed by ethyl alcohol precipitation, yielded a crude polysaccharide (TO_{SP}), comprising 5.40 % of the dry weight (Table 1). The crude polysaccharide comprised 64.07 % total sugars, 15.25 % sulfate, and 5.01 % uronic acid (Table 1). The elution profile of crude polysaccharide (TO_{SP}) from DEAE-cellulose chromatography is shown in Fig. S1. Among the eluted fractions (TO_{SP}-0 to TO_{SP}-5), TO_{SP}-3 demonstrated the highest carbohydrate content (73.25 %), along with substantial sulfate (18.02 %), suggesting a complex and highly polyanionic structure. This aligns with the previous report of sulfated rhamnogalactofucan from the brown seaweed, *Eclonia cava* [36] and polygalacto-fucopyranose isolated from *Sargassum wightii* [25], both of which exhibited similar sulfate content. Consequently, TO_{SP}-3 was selected for further spectroscopic analysis and bioactivity evaluations. The analysis of monosaccharide composition in the hydrolyzed TO_{SP}-3 fraction demonstrated a predominant occurrence of fucose (79.90 %) and galactose (20.10 %) as the primary repeating units indicating their significant contribution to the polysaccharide structure (Fig. S2). These findings are in agreement with earlier studies on the monosaccharide composition of *T. ornata*, which indicated a fucose-to-galactose ratio of approximately 3:1 [37].

3.3. Spectral characterization of TO_{SP}-3

The structural characterization of TO_{SP}-3 was elucidated by spectroscopic techniques, including FTIR, nuclear magnetic resonance (NMR), {HR(ESI)MS}, and GC–MS. FTIR analysis (Fig. 1A) was performed as an initial step in elucidating the complex structure of the polysaccharide, providing functional insights into its molecular framework. A broad absorption signal at 3389 cm^{-1} was typically indicative of O—H stretching, while the peaks between 2853 cm^{-1} and 2989 cm^{-1} were attributed to the C—H stretching of the pyranoid rings and the C-6 (CH_2) groups of TO_{SP}-3. Furthermore, medium to strong infrared signals ranging 1200 cm^{-1} to 970 cm^{-1} were ascribed to the stretching frequencies of C–O–C associated with glycosidic bonds, as well as the C-C/

Table 1
Yield and biochemical composition of crude polysaccharide (TO_{SP}) and eluted column fractions (TO_{SP}-0 to TO_{SP}-5) from *T. ornata*.

Biochemical [†]composition	TO_{SP}	TO_{SP}-0	TO_{SP}-1	TO_{SP}-2	TO_{SP}-3	TO_{SP}-4	TO_{SP}-5
[†]Yield	$5.40^{f} \pm 0.02$	$2.21^{g} \pm 0.02$	$14.21^{c} \pm 0.02$	$11.61^{e} \pm 0.02$	$26.24^{a} \pm 0.02$	$18.96^{b} \pm 0.02$	$12.01^{d} \pm 0.02$
[‡]Total carbohydrate	$64.07^{b} \pm 0.19$	$2.05^{f} \pm 0.07$	$4.19^{e} \pm 0.18$	$28.01^{c} \pm 0.13$	$73.25^{a} \pm 0.59$	$5.13^{d} \pm 0.21$	$4.02^{e} \pm 0.16$
[‡]Uronic acid	$5.01^{b} \pm 0.16$	$0.25^{f} \pm 0.05$	$3.80^{e} \pm 0.1$	$4.95^{c} \pm 0.16$	$5.89^{a} \pm 0.09$	$4.83^{d} \pm 0.09$	$3.15^{e} \pm 0.09$
[‡]Sulfate	$15.25^{b} \pm 0.17$	$0.67^{e} \pm 0.18$	$2.01^{d} \pm 0.15$	$12.04^{c} \pm 0.21$	$18.02^{a} \pm 0.15$	$2.08^{d} \pm 0.30$	$0.78^{e} \pm 0.07$

The samples were analyzed in quadruple replicates ($n = 4$) and expressed as mean ± standard deviation.
Significant differences ($p < 0.05$) between means were indicated by assigning different superscript letters (a–g) within the same row.
[†] Yield and biochemical composition were recorded as % w/w.
[‡] Total carbohydrate, uronic acid and sulfate contents were expressed as % *w*/w.

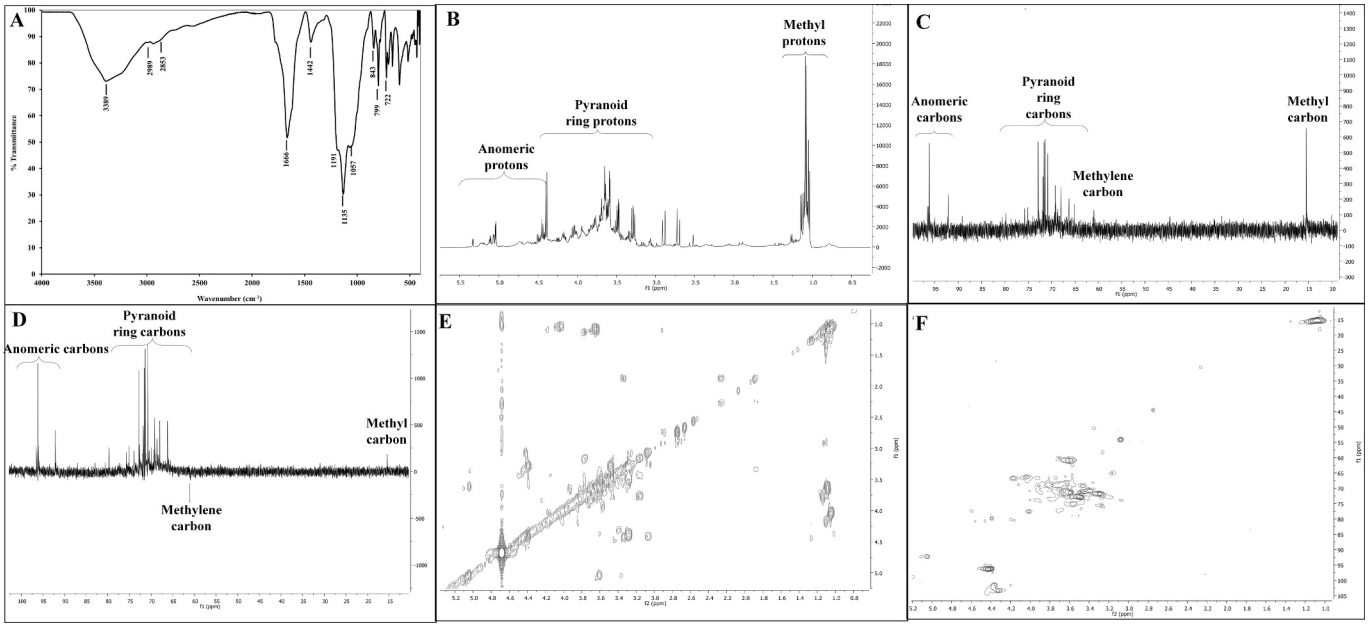

Fig. 1. Spectral analysis of TO_{SP}-3: (A) FTIR spectrum, (B) ^{1}H NMR, (C) ^{13}C NMR, (D) DEPT-135, (E) ^{1}H-^{1}H COSY, and (F) HSQC spectra.

C-O stretching modes within the pyranose moieties [38]. The absorption signal at 1442 cm^{-1} was attributed to bending vibration representing the methyl group of Fuc*p* [39]. The intense infrared signal at 1191 cm^{-1} was indicative of S═O stretching associated with the sulfate moieties of TO_{SP}-3. A distinct peak at 843 cm^{-1} corresponded to the bending vibration of C-O-S of secondary axial sulfate occurring at the C-4 position of TO_{SP}-3 [40]. The absorption signal at 1057 cm^{-1} represented the C—O symmetrical vibration associated with a C–O–SO_3 moiety [41].

The NMR spectroscopic details representing the monosaccharides, *α*-fucopyranose (unit A) and *β*-galactopyranose (unit B) in TO_{SP}-3 are provided in Table 2. The proton NMR spectrum (Fig. 1B) revealed two characteristic doublet peaks in the anomeric region at δ_H 5.04 ($J = 3.9$ Hz) and δ_H 4.40 ($J = 8.0$ Hz), which are attributed to the anomeric protons of the Fuc*p* and Gal*p* subunits, respectively. The anomeric hydrogen exhibiting a chemical shift (δ) above δ_H 5.0 ppm and below 5.0 ppm was identified as *α*- and *β*-configurations, respectively. Furthermore, the *β*- anomeric hydrogen typically shows a coupling constant of 7–9 Hz, indicating a trans-diaxial relationship, whereas for the *α*-configuration, the smaller coupling constant of 2–4 Hz reflects a gauche or axial-equatorial interaction [19,42]. Chemical shifts ranging from δ_H 3.30–4.39 ppm accredited to C-2 to C-6 pyranoid ring protons of *α*-Fuc*p* and *β*-Gal*p* moieties. Additionally, the intense peak at δ_H 1.09 ppm was ascribed to methyl protons of *α*-Fuc*p*.

The distinct signals at δ_C 92.2 and 96.2 ppm in the ^{13}CNMR spectrum (Fig. 1C) represented the anomeric carbons of *α*-Fuc*p*, and *β*-Gal*p*, respectively. The chemical shifts of pyranoid ring carbons C2-to C-5 ranged between δ_C 69.2–80.6 ppm. The intense carbon peak (Fig. 1C) at δ_C 15.5 ppm was assigned to the methyl group of *α*-Fuc*p* residue. The ^{13}C peak (Fig. 1C) at δ_C 60.9 ppm, which was observed in negative phase of DEPT-135 (Fig. 1D), was attributed to the methylene carbon (C-6) of *β*-Gal*p* subunit [19]. The sequential assignment of ring protons was deduced from the cross peaks in the ^{1}H-^{1}H COSY spectrum (Fig. 1E). The COSY spectrum displayed the correlations of AH1/AH2 ($\delta_{H/H}$ 5.04/3.30 ppm), AH2/AH3 ($\delta_{H/H}$ 3.30/3.47 ppm), AH3/AH4 ($\delta_{H/H}$ 3.47/4.39 ppm), AH4/AH5 ($\delta_{H/H}$ 4.39/3.65 ppm), and AH5/AH6 ($\delta_{H/H}$ 3.65/1.09 ppm) of the *α*-Fuc*p* subunit. The ^{1}H—^{1}H correlations of BH1/BH2/BH3/BH4/BH5/BH6 ($\delta_{H/H}$ 4.40/3.35/3.49/4.17/4.03/3.66 ppm) of *β*-Gal*p* are depicted in the COSY spectrum (Fig. 1E). Further, the ^{1}H—^{13}C correlations of H1/C1 and H6/C6 of *α*-Fuc*p*, and *β*-Gal*p* units are supported by strong HSQC cross peaks (Fig. 1F) at $\delta_{H/C}$ 5.04/92.2 ppm (AH1/AC1), $\delta_{H/C}$ 1.09/15.5 ppm (AH6/AC6), and $\delta_{H/C}$ 4.40/96.2 ppm (BH1/BC1), $\delta_{H/C}$ 3.66/60.9 ppm (BH6/BC6), respectively, along with other HSQC

Table 2
[‡]NMR spectroscopic details of TO_{SP} -3.

[→3)- 4-*O*-SO_3^--*α*-Fuc*p*-(1 → 3)-4-*O*-SO_3^--*β*-Gal*p*-(1→]		
$^{1}H/^{13}C$	4-*O*-SO_3-*α*-fucopyranose (Unit A)	4-*O*-SO_3-*β*-galactopyranose (Unit B)
H1/C1	5.04/92.2	4.40/96.2
H2/C2	3.30/72.0	3.35/70.8
H3/C3	3.47/69.2	3.49/72.9
H4/C4	4.39/79.8	4.17/80.6
H5/C5	3.65/71.4	4.03/69.2
H6/C6	1.09/15.5	3.66/60.9

[‡] Spectral data were obtained on an NMR spectrometer utilizing D_2O as the solvent, with chemical shifts (δ) reported in ppm.

correlations at $\delta_{H/C}$ 3.30/72.0 ppm (AH2/AC2), $\delta_{H/C}$ 3.47/69.2 ppm (AH3/AC3), $\delta_{H/C}$ 4.39/79.8 ppm (AH4/AC4), $\delta_{H/C}$ 3.65/71.4 ppm (AH5/AC5), $\delta_{H/C}$ 3.35/70.8 ppm (BH2/BC2), $\delta_{H/C}$ 3.49/72.9 ppm (BH3/BC3), $\delta_{H/C}$ 4.17/80.6 ppm (BH4/BC4), and $\delta_{H/C}$ 4.03/69.2 ppm (BH5/BC5). The downfield peaks at $\delta_{H/C}$ 4.39/79.8 ppm (AH4/AC4) and $\delta_{H/C}$ 4.17/80.6 (BH4/BC4) further confirmed the sulfate substitution in the C-4 position of *α*-Fuc*p* and *β*-Gal*p* with deshielding due to the electron-withdrawing effect. The HMBC spectrum (Fig. S3) exhibited intra-residual correlations between AH3/AC2 ($\delta_{H/C}$ 3.47/72.0 ppm), AH5/AC6 ($\delta_{H/C}$ 3.65/15.5 ppm), and AH6/AC5 ($\delta_{H/C}$ 1.09/71.4 ppm) of the *α*-Fuc*p* moiety, as well as BH6/BC5 ($\delta_{H/C}$ 3.66/69.2 ppm) of galactopyranose, thereby confirming their proximity.

Glycosidic linkage between *α*-Fuc*p* and *β*-Gal*p* was established by analyzing fragmentation patterns of PMAAs (Fig. S4). Subsequent to sequential chemical derivatization, the resulting alditol acetates of the monosaccharides, 2,3-dimethoxy-1,4,5-triacetoxy-fucitol, and 1,2,6-trimethoxy-3,4,5-triacetoxy-galactitol were confirmed by the GC–MS spectroscopy. The fragment of 1,2,6-trimethoxy-3,4,5-triacetoxy-galactitol corresponding to the signal at *m/z* 233 is produced by the cleavage of the C4-C5 bond. The spectra included *m/z* 161 and 189 signals ascribed to the fragment obtained from the breakage of C3-C4 bonds. The fragment $(AcO\text{-}CH_2\text{-}CH\text{-}OMe)^+$ corresponded to the post cleavage of 2,3-dimethoxy-1,4,5-triacetoxy-fucitol and 1,2,6-trimethoxy-3,4,5-triacetoxy-galactitol, yielding a peak at *m/z* 117. Additional significant peaks at *m/z* 87 and 73 resulted from the cleavage of the C4-C5 and C1-C2 bonds, respectively in 2,3-dimethoxy-1,4,5-triacetoxy-fucitol. The peak at *m/z* 89 corresponded to the fragment formed by the cleavage of the C2-C3 bond in 1,2,6-trimethoxy-3,4,5-triacetoxy-galactitol. The HR (ESI)MS spectrum (Fig. S5) revealed the molecular ion signal at *m/z* 1003.6791 $[M\text{-}H]^-$ that is attributed to the oligosaccharide [→3)-*α*-Fuc*p*-(1 → 3)-*β*-Gal*p*-(1 → 3)-4-*O*-SO_3H-*α*-Fuc*p*-(1 → 3)-4-*O*-SO_3H-*β*-Gal*p*-(1 → 3)-4-*O*-SO_3H-*α*-Fuc*p*]. Other major peaks at *m/z* 713.5061, 791.5140 and 792.5171 can be accredited to fragments [4-*O*-SO_3H-*α*-Fuc*p*-(1 → 3)-*β*-Gal*p*-(1 → 3)-*α*-Fuc*p*-(1 → 3)-*β*-Gal*p*], [4-*O*-SO_3-*α*-Fuc*p*-(1 → 3)-*β*-Gal*p*-(1 → 3)-*α*-Fuc*p*-(1 → 3)-4-*O*-SO_3-*β*-Gal*p*]$^{2-}$, and [4-*O*-SO_3H-*α*-Fuc*p*-(1 → 3)-*β*-Gal*p*-(1 → 3)-*α*-Fuc*p*-(1 → 3)-4-*O*-SO_3-*β*-Gal*p*]$^-$, respectively. The elucidated structural linkage and sulfation pattern of TO_{SP}-3 are in correlation with earlier reports [37,43]. According to these findings, the putative structure of TO_{SP}-3 was deduced as a polysaccharide comprising [→3)-4-*O*-SO_3-*α*-Fuc*p*-(1 → 3)-4-*O*-SO_3-*β*-Gal*p*-(1→] as major units.

3.4. Preliminary antioxidant activities of TO_{SP}-3

The antioxidant potential of TO_{SP}-3 was assessed through in vitro radical decolorization assays, measuring its capability to neutralize DPPH• and $ABTS^+$ radicals. The isolated polysaccharide TO_{SP}-3 exhibited greater DPPH• and $ABTS^+$ quenching activity (IC_{50} 0.19 mg/mL and 0.15 mg/mL, respectively), compared to *α*-tocopherol {IC_{50} 0.24 mg/mL (DPPH•) and 0.22 mg/mL ($ABTS^+$), respectively} (Table S1).

Previous studies have shown that fucoidans effectively neutralize reactive oxygen species (ROS), enhance antioxidant activity, and facilitate H_2O_2 decomposition. Fucoidan isolated from *Undaria pinnatifida* sourced from New Zealand was found to exhibit superior antioxidant efficacy compared to the butylated hydroxyanisole (BHA), while *Sargassum binderi* derived fucoidan (Fsar) surpasses synthetic antioxidants (BHA) [4]. Given the strong antioxidant potential of fucoidans, their role in mitigating oxidative stress-induced disorders, such as thrombosis, warrants further investigation. Oxidative stress is acknowledged as a key contributor to the development of thrombosis, primarily by virtue of the overproduction of reactive oxygen species (ROS) that overwhelm the intrinsic antioxidant defenses of the body. Excessive ROS levels have been implicated in the upregulation of tissue factor expression within endothelial cells, arterial smooth muscle cells, and monocytes, thereby triggering coagulation cascades [44]. Furthermore, ROS disrupt the delicate equilibrium of platelet activation and induce modifications in key coagulation proteins, such as fibrinogen and antithrombin, thereby exacerbating pro-thrombotic states [44,45]. The potent radical quenching capability of TO_{SP}-3, evidenced by its superior DPPH• and $ABTS^+$ free radical neutralization (IC_{50} ~0.17 mg/mL), suggests a mechanistic pathway through which this sulfated polysaccharide may exert anticoagulant effects. The enhanced radical-scavenging activity of TO_{SP}-3 can be correlated to the presence of strongly reactive polar entities and negatively charged functional groups, specifically hydroxyl (-OH) and sulfate ($-OSO_3^-$) moieties. These functional groups not only facilitate efficient electron donation but also promote the stabilization of free radicals, potentially mitigating ROS-induced coagulation pathways [46,47]. Moreover, previous literature described that greater sulfate content within sulfated polysaccharides could be correlated with a marked increase in antioxidant potencial, thereby reinforcing the critical influence of sulfation patterns on their bioactivity [48]. Sellimi et al. (2014) revealed that the distinct sulfation pattern of polysaccharides markedly enhances their antioxidant properties, with a pronounced effect observed when sulfate moieties are positioned at the C-4 carbon [49]. Dore et al. (2012) studied the anticoagulant and antioxidant activities of a sulfated polysaccharide from the brown seaweed *Sargassum vulgare*, which contains about 37 % fucose, and exhibited 22.2 % antioxidant activity at a concentration of 2.5 mg/mL [50]. In contrast, TO_{SP}-3, which has a much higher fucose content (~80 %), exhibited 50 % antioxidant activity at a significantly lower concentration of 0.19 mg/mL. In another study by Ma et al. (2017), a polysaccharide isolated from the seaweed *Porphyra yezoensis* showed a two-fold lower antioxidant efficiency (IC_{50} = 1.82 mg/mL) compared to the control [47]. Moreover, when compared to the standard antioxidant *α*-tocopherol (IC_{50} = 0.24 mg/mL), TO_{SP}-3 exhibited 1.26 times stronger scavenging activity, further emphasizing its antioxidant potential. The superior antioxidant potential of TO_{SP}-3 can be attributed to its high fucose (~80 %) and sulfate (~18 %) contents, which enhance electron-donating capacity and stabilize free radicals, thereby reducing the oxidative damage. Building on these findings, we proceeded to evaluate the anticoagulant effects of TO_{SP}-3 on HUVECs, further investigating its potential therapeutic applications in oxidative stress-related thrombosis.

3.5. Effects of sulfated galactofucan on aPTT and PT

The anticoagulant effects of isolated polysaccharide TO_{SP}-3 on both intrinsic and extrinsic mechanisms of the blood coagulation cascade were assessed based on activated partial thromboplastin time (aPTT) and prothrombin time (PT) assays in normal human plasma. The findings revealed that TO_{SP}-3 significantly prolonged the clotting time for both aPTT and PT assays in a dose-dependent manner (6.25–25 μg/mL, $p < 0.05$). Notably, at 25 μg/mL, TO_{SP}-3 induced a notable delay in aPTT by 3.79-fold, resulting in a clotting time of 100.49 s, while also extending PT by 3.34-fold (77.57 s), relative to the control group (PBS, phosphate buffer saline) (Fig. 2A-B) (Table 3). In contrast, fucoidan isolated from cloned *Grateloupia filicina* exhibited a lower anticoagulant effect, increasing aPTT by only 2.5-fold at a higher concentration of 30 μg/mL, compared to the control. Similarly, *Fucus vesiculosus* derived fucoidan extended clotting time of PT assay from 13.3 s (control) to 15.2 s at 80 μg/mL [51,52]. While heparin exhibits anticoagulant activity by extending aPTT (1.49-fold) and PT (1.39-fold) compared to TO_{SP}-3 (25 μg/mL), its clinical use is often restricted due to potential bleeding complications and heparin-induced thrombocytopenia (HIT) [13].

The aPTT and PT serve as essential assays that are used to study the intricate mechanisms of blood coagulation. The aPTT assay evaluates the intrinsic pathway, encompassing factors VIII, IX, XI, and XII as well as common pathways, which includes factors I, II, V, and X by measuring the time taken for clot formation. In contrast, the PT assay evaluates the extrinsic pathway, particularly factor VII, along with the common pathway by measuring clotting time in response to tissue factor [9]. The

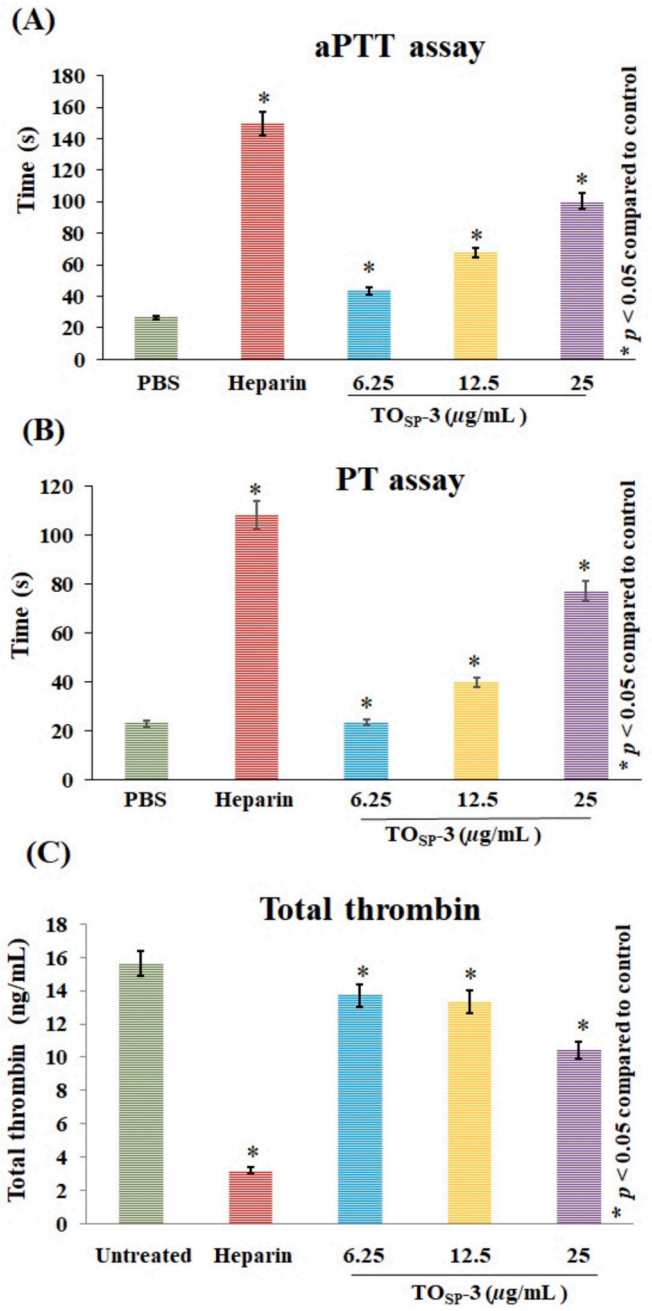

Fig. 2. (A-B) In vitro anticoagulant effects of TO_{SP}-3. (A) activated partial thromboplastin time (aPTT) and (B) prothrombin time (PT). Phosphate buffer saline (PBS) served as control ($p < 0.05$). (C) Total thrombin production by TO_{SP}-3 in HUVECs.

more pronounced effect of TO_{SP}-3 on aPTT, as compared to PT, is consistent with previous findings, wherein the sulfated polysaccharide derived from the brown algae, *Cystoseira myrica*, predominantly influenced the intrinsic coagulation pathway [51]. Further, previous literature indicated that sulfated polysaccharides derived from *Fucus vesiculosus* and Tasmanian *Undaria pinnatifida* demonstrated minimal effects on PT at lower concentrations, but displayed anticoagulant activity at elevated concentrations [51,52]. Interestingly, the present study demonstrated a significant prolongation of both aPTT and PT by TO_{SP}-3 (Table 3), suggesting a multifaceted mechanism of action that may influence both intrinsic and extrinsic coagulation pathways. This suggests that TO_{SP}-3 affects key coagulation factors, such as factors XII, XI, IX, which are known to extend aPTT, as well as factor VII and tissue factor, which influence PT extension. Furthermore, the presence of sulfated moieties on TO_{SP}-3 enhances the overall negative charge of the polysaccharide, thereby facilitating interactions with positively charged coagulation factors, such as factors VIII, IX, XI, and XII. This interaction likely interferes with the normal functioning of these factors, resulting in prolonged blood clotting times, as evidenced by the aPTT assays [42,53].

3.6. Cell-line based anticoagulant effects of sulfated galactofucan TO_{SP}-3

3.6.1. Cytotoxicity assessment of TO_{SP}-3

The cytotoxicity analysis of the isolated sulfated galactofucan TO_{SP}-3 on HUVECs at varied dosages (6.25 to 100 μg/mL) was conducted using the MTT assay. The results revealed that TO_{SP}-3 exhibited no cytotoxic effect on HUVECs, even at higher concentrations. At 6.25 μg/mL, over 96 % of the cells remained viable after 24 h of treatment, and >87 % viability was maintained after 72 h (Fig. S6-S9; Table S2). Even at higher concentrations (25, 50, and 100 μg/mL), 75 % cell viability was noted, significantly higher than the cell viability (~50 %) observed with heparin treatment (Fig. S9). Moreover, TO_{SP}-3-treated cells retained their characteristic spherical morphology, with no observable detriment to cellular growth or proliferative capacity. Based on these findings, three lower dosages (6.25, 12.5, and 25 μg/mL) were chosen for subsequent anticoagulant assessments in HUVECs.

3.6.2. Effects of sulfated galactofucan TO_{SP}-3 on total thrombin production

The anticoagulant properties of TO_{SP}-3 on total thrombin production in HUVECs were assessed using the ELISA method. The data displayed a marked ($p < 0.05$) dose-dependent (6.25–25 μg/mL) decrease in thrombin production in response to TO_{SP}-3 treatment compared to untreated cells (Table 3). A moderate reduction in thrombin levels, ranging from 12.3 % to 14.7 %, was observed with the co-administration of TO_{SP}-3 at lower dosages (6.25 and 12.5 μg/mL). Conversely, the elevated dosage of TO_{SP}-3 (25 μg/mL) led to a more pronounced decrease ($p < 0.05$), with a marked reduction of 33.2 % relative to the control (untreated cells) (Fig. 2C; Table 3).

Thrombin (clotting factor IIa), an endolytic serine protease, plays a crucial role in the coagulation cascade by catalyzing the conversion of fibrinogen to fibrin, which forms a fibrous mesh that stabilizes the blood clot. It also activates several other coagulation factors, such as factors V, VIII, and XI, enhancing the clotting response [54]. Previous research on

Table 3
Anticoagulation activity of TO_{SP}-3 measured by aPPT and PT assays and total thrombin production in HUVECs.

Sample	Dose (μg/mL)	aPPT (s)	Fold increase	PT (s)	Fold increase	Total thrombin (ng/mL)	Percentage decrease
[†]Control	–	$26.50^{e} \pm 2.16$	1	$23.20^{d} \pm 0.40$	1	$15.62^{a} \pm 1.01$	–
Heparin	6.25	$149.71^{a} \pm 3.71$	5.65	$108.50^{a} \pm 1.50$	4.68	$3.22^{d} \pm 0.77$	79.43
TO_{SP}-3_A	6.25	$43.36^{d} \pm 0.98$	1.63	$23.55^{d} \pm 0.15$	1.01	$13.70^{b} \pm 0.99$	12.39
TO_{SP}-3_B	12.5	$67.63^{c} \pm 0.79$	2.56	$39.89^{c} \pm 1.44$	2.72	$13.32^{b} \pm 0.94$	14.61
TO_{SP}-3_C	25	$100.49^{b} \pm 1.93$	3.79	$77.57^{b} \pm 1.09$	3.34	$10.44^{c} \pm 0.82$	33.18

The samples were analyzed in quadruple replicates (n = 4) and presented as mean ± standard deviation.
Means accompanied by superscripts (a-e) in the same column denote significant differences ($p < 0.05$).
[†] Phosphate buffer saline (PBS) served as control for aPPT and PT assays; Untreated cells were used as control for total thrombin production.

fucoidan isolated from *Cystoseira myrica* (FCm) reported no inhibition of thrombin [51]. In contrast, the observed reduction in total thrombin production upon treatment with TO_{SP}-3 suggests a potential inhibition of thrombin activity, thereby reinforcing its anticoagulant properties. Sulfated polysaccharides augment anticoagulation by facilitating the formation of complexes between thrombin and its endogenous inhibitors, including antithrombin III (ATIII) and heparin cofactor II (HCII). This interaction effectively obstructs the catalytic site of thrombin, leading to a pronounced inhibitory effect. The strong binding interaction of sulfated polysaccharides for HCII further enhances thrombin inhibition, leading to a notable reduction in thrombin levels [42,55–57]. Previous clinical and in vitro investigations have corroborated the thrombin inhibitory properties of fucoidan, with notable alterations in thrombin time observed by post-administration [58]. In the context of HCII-dependent suppression, the key structural integrity of the sulfated polysaccharide is critical, particularly the fucose residues with 4-*O* sulfation, which are essential for the anticoagulant activity. Furthermore, (1 → 3)-linked linear chain of *α*-L-fucans abundant in residues with disulfation at C-2, C-4 positions have been demonstrated to significantly enhance the anticoagulant activity mediated by ATIII [59,60]. Sulfated polysaccharides extracted from several seaweeds, such as *Fucus vesiculosus* and *Laminaria brasiliensis*, have demonstrated direct thrombin inhibition, characterized by structures composed of *α*-L-fucose residues arranged in alternating (1 → 3) and (1 → 4) linkages, which are sulfated at the C-2/C-4 positions and often feature branching fucose units [61]. Similar inhibitory mechanisms have also been observed in sulfated polysaccharides from *Saccharina latissima* and *Fucus distichus* [62]. In this context, TO_{SP}-3, characterized by its 4-*O*-sulfated (1 → 3)-linked *α*-fucopyranosyl backbone and high sulfate content, shows enhanced anticoagulant activity due to these multifaceted mechanisms.

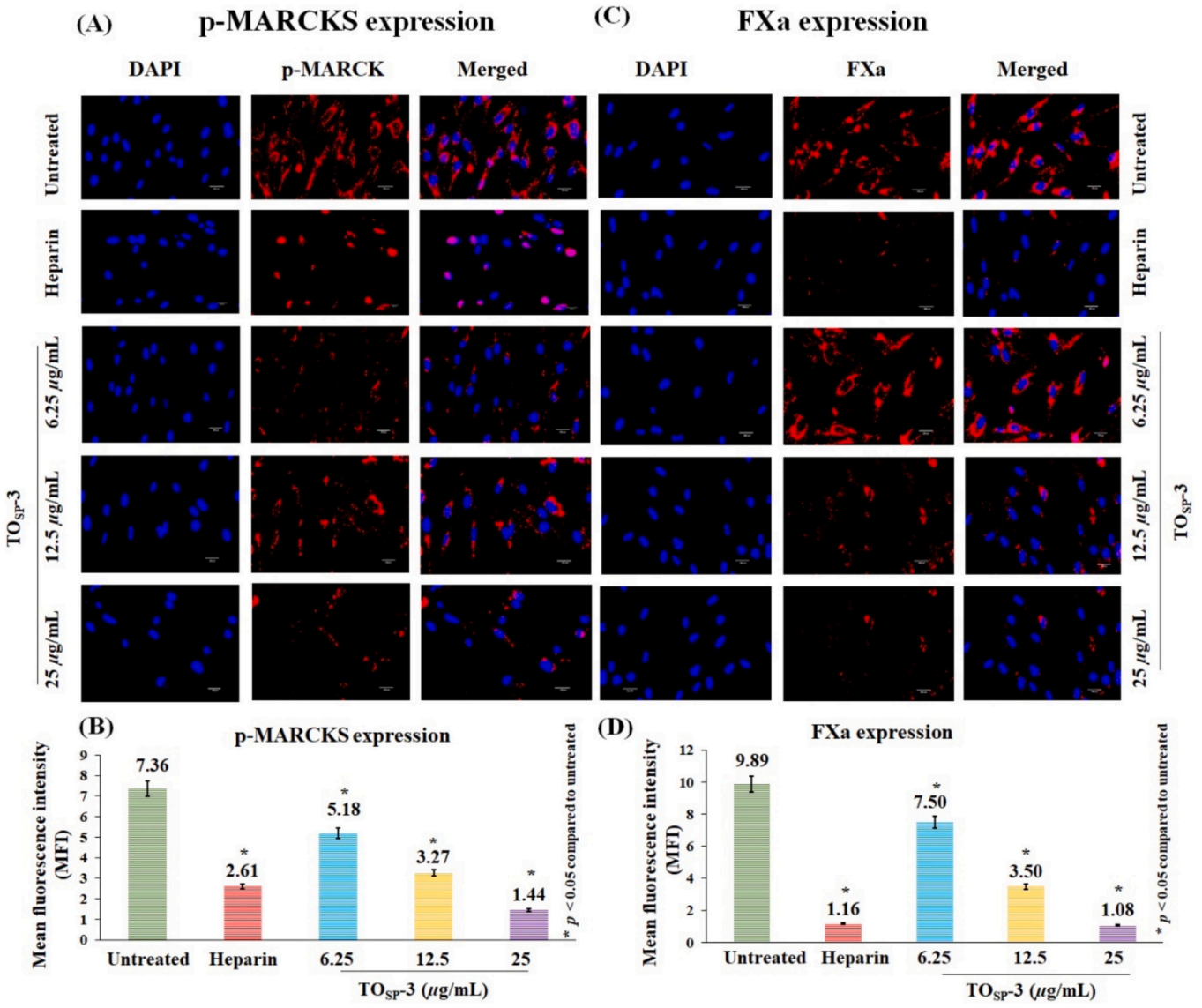

Fig. 3. (A) Expression of phospho-MARCKS on following treatment with TO_{SP}-3 and heparin in HUVECs. The p-MARCKS expression on untreated, heparin (6.25 μg/mL), and TO_{SP}-3-treated (6.25, 12.5, and 25 μg/mL) cells appeared red, whereas DAPI stained cells appeared blue. The recovery effect of TO_{SP}-3 on p-MARCKS expression was exhibited by the reduced number of red-coloured cells compared to untreated HUVE cells. (B) Mean fluorescence intensity of p-MARCKS expression following treatment with TO_{SP}-3 (6.25, 12.5, and 25 μg/mL) and heparin (6.25 μg/mL) compared to untreated HUVE cells. (C) Following treatment with TO_{SP}-3 and heparin in HUVECs, the factor Xa expression on untreated, heparin (6.25 μg/mL), and TO_{SP}-3 treated (6.25, 12.5, and 25 μg/mL) cells appeared red, whereas DAPI stained cells appeared blue. The recovery effect of TO_{SP}-3 on factor Xa expression was exhibited by reduced number of red-coloured cells compared to untreated HUVE cells. (D) Mean fluorescence intensity of factor Xa expression following treatment with TO_{SP}-3 (6.25, 12.5, and 25 μg/mL) and heparin (6.25 μg/mL) compared to untreated HUVEC cells.

3.6.3. Effects of TO_{SP}-3 on p-MARCKS and coagulation factor FXa expression

The effect of TO_{SP}-3 on p-MARCKS and factor Xa (FXa) expression in HUVECs were analyzed using fluorescence microscopy (Fig. 3). The analysis revealed a concentration-dependent ($p < 0.05$) decrease in p-MARCKS expression following treatment with TO_{SP}-3 (6.25–12.5 μg/mL). Treatment with 6.25 μg/mL TO_{SP}-3 resulted in a modest reduction in fluorescence intensity, corresponding to a 43 % decrease compared to untreated control cells. Increasing the concentration to 12.5 μg/mL yielded a more pronounced effect, with fluorescence intensity diminishing by 61 %. The highest concentration of TO_{SP}-3 (25 μg/mL) caused a substantial downregulation of p-MARCKS expression, characterized by a decline in fluorescence intensity exceeding 80 % (Fig. 3A-B). The decrease in fluorescence corresponding to p-MARCKS expression indicates that TO_{SP}-3 effectively downregulates p-MARCKS in HUVECs, potentially contributing to its anticoagulant activity by modulating endothelial cell signaling pathways.

Similarly, a systematic reduction in FXa expression, as indicated by red fluorescence intensity measurements ($p < 0.05$), was noted following treatment with increasing concentrations of TO_{SP}-3. At 6.25 μg/mL, FXa expression decreased by 24.2 % compared to the untreated control. This reduction became more pronounced at 12.5 μg/mL, where FXa levels dropped by 64.7 %. Furthermore, at maximum concentration of 25 μg/mL, FXa expression was diminished significantly by 89.13 % (Fig. 3C-D). These collective results suggest that TO_{SP}-3 exerts a profound influence on FXa expression, potentially contributing to its anticoagulant properties.

FXa, a pivotal serine endopeptidase in the coagulation cascade, catalyzes the conversion of prothrombin to thrombin, which subsequently facilitates the transformation of fibrinogen into fibrin, a critical step in clot formation [63]. The observed downregulation of FXa expression following TO_{SP}-3 treatment suggests a potential disruption of this coagulation pathway, thereby presenting an innovative strategy for the prevention of thrombosis and its associated vascular complications. Previous studies on sulfated polysaccharides derived from *Ecklonia kurome* have defined their significant ability to inhibit FXa generation, highlighting its potential as an anti-coagulant agent for mitigating clot-related disorders [64]. The increased sulfation in polysaccharides is known to enhance their negative charge density, thereby improving their interactions with key clotting proteins, such as thrombin and factor Xa, resulting in more pronounced inhibitory effects and extended coagulation times [65]. Previous research on a sulfated galactofucan from *Sargassum plagiophyllum* (SP2), demonstrated anticoagulant activity by reducing p-MARCKS expression by 84 % and FXa expression by 86 % at 25 μg/mL, along with a two-fold decrease in mean fluorescence intensity (1.16 MFI) compared to heparin (2.60 MFI) [32]. In comparison, TO_{SP}-3 exhibited a more pronounced anticoagulant effect, with an over 80 % reduction in p-MARCKS expression and an 89.13 % decrease in FXa levels at the same concentration. These findings suggest that TO_{SP}-3 exhibits superior anticoagulant properties over SP2, offering more effective modulation of coagulation pathways. A similar anticoagulant mechanism has been reported in 4-*O* sulfated polysaccharides from *Sargassum polycystum*, which exhibited moderate FXa inhibition [60]. Similarly, TO_{SP}-3, with its 4-*O* sulfated fucoidan having elevated sulfate content, enhances anticoagulant properties by effectively suppressing Factor Xa, further corroborating its potential therapeutic implications in anticoagulation. Similar to heparin, which acts by enhancing antithrombin III (ATIII) activity, TO_{SP}-3 appears to function through a direct suppression of FXa expression, representing a distinct anticoagulant mechanism. Additionally, unlike heparin, which is associated with thrombocytopenia and hemorrhagic risks, TO_{SP}-3 demonstrated a safer profile, as indicated by no significant cytotoxicity in HUVECs.

3.6.4. Effect of TO_{SP}-3 on intracellular Ca^{2+} levels in HUVECs

Intracellular Ca^{2+} mobilization in HUVECs was evaluated using fluorimetry to assess the anticoagulant properties of TO_{SP}-3 on thrombin-induced calcium levels (Fig. 4A). Treatment with TO_{SP}-3 (25 μg/mL) significantly reduced thrombin-induced calcium elevation, as indicated by a 20.4 % decrease in intracellular Ca^{2+} levels measured after 140 min. This inhibitory effect was even more pronounced, when measured at 260 min, with a 32.85 % decrease in Ca^{2+} levels compared to cells treated with thrombin alone. These findings demonstrate that TO_{SP}-3 effectively suppresses the elevation in thrombin-induced Ca^{2+} levels, emphasizing its potential as a potent modulator of thrombin-mediated calcium signaling pathways.

Thrombin, an essential enzyme within the coagulation cascade, initiates an elevation in intracellular calcium levels by activating protease-activated receptors (PARs), which subsequently stimulates the release of calcium from the endoplasmic reticulum [66]. In this context, TO_{SP}-3 appears to hinder the interaction between thrombin and PARs, thereby attenuating the subsequent calcium release and potentially modulating calcium ion channels to inhibit calcium influx. This mechanism suggests that TO_{SP}-3 effectively disrupts calcium-dependent coagulation pathways, thereby enhancing its anticoagulant properties. Furthermore, analogous studies have demonstrated that sulfated polysaccharides derived from *Laminaria japonica* can effectively suppress platelet activation by reducing calcium influx within the cells [67]. Based on these findings, TO_{SP}-3 may possess the dual capacity to inhibit thrombin-induced calcium release while simultaneously reducing calcium influx, positioning it as a promising agent in modulating calcium-dependent coagulation pathways and the regulation of platelet activation.

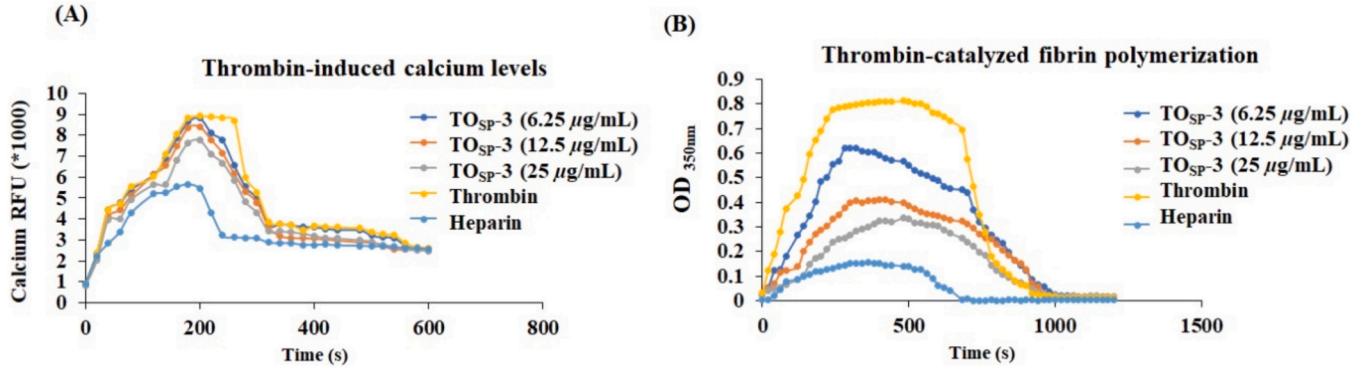

Fig. 4. Effects of TO_{SP}-3 and heparin on thrombin-induced intracellular calcium levels and thrombin production in HUVECs. (A) Intracellular calcium levels in HUVECs following thrombin stimulation and treatment with TO_{SP}-3 (6.25, 12.5, and 25 μg/mL) and heparin (6.25 μg/mL). (B) Inhibition of thrombin-catalyzed fibrin polymerization by TO_{SP}-3 (6.25, 12.5, and 25 μg/mL) and heparin (6.25 μg/mL).

3.6.5. Effect of TO_{SP}-3 on thrombin-catalyzed fibrin polymerization

The evaluation of thrombin-induced fibrin polymerization indicated a pronounced inhibitory effect of TO_{SP}-3 on fibrin formation. Specifically at 20 s interval, treatment with TO_{SP}-3 (at 25 μg/mL) resulted in a noteworthy 67.7 % reduction in fibrin formation, the inhibition was further increased to 82.3 % measured at 80 s interval. These results demonstrate that TO_{SP}-3 effectively inhibits thrombin-mediated fibrin polymerization in a dos-dependent manner ($p < 0.05$), with higher concentrations leading to progressively greater reductions in fibrin formation (Fig. 4B).

Thrombin-catalyzed fibrin polymerization is essential for blood clotting, converting soluble fibrinogen into insoluble fibrin, a fundamental step in clot formation that prevents excessive hemorrhage [10]. Thrombin, a serine protease, initiates this conversion by cleaving fibrinogen to release fibrinopeptides A and B, which subsequently yield soluble fibrin monomers that undergo polymerization to form protofibrils. These protofibrils aggregate to create a robust three-dimensional fibrin network, a structure further reinforced by thrombin-activated factor XIII, which interconnects fibrin strands to enhance the stability of the clot [62]. The significant inhibition of fibrin polymerization by TO_{SP}-3 showed its ability to disrupt the function of thrombin, effectively impeding its capacity to facilitate fibrinogen conversion into fibrin, a pivotal mechanism in hemostasis [68,69]. Furthermore, the sulfated moieties of TO_{SP}-3 enhances its interaction with thrombin, likely resulting from the electrostatic attraction involving the anionic sulfate groups and the cationic regions of the enzyme, thus enhancing its anticoagulant efficacy.

3.6.6. Effect of TO_{SP}-3 on ADP-induced platelet aggregation

The anti-platelet aggregation properties of TO_{SP}-3 were assessed using a spectrophotometry method, with ADP (10 μM) stimulated platelet aggregation. TO_{SP}-3 exhibited a pronounced, dose-responsive inhibition of platelet aggregation induced by the ADP agonist. At lowest concentration of 6.25 μg/mL, TO_{SP}-3 achieved a modest reduction in platelet aggregation, diminishing it to 96.81 % relative to the control. This inhibitory effect became more substantial at 12.5 μg/mL, where aggregation levels were reduced to 91.57 %. Notably, the most significant suppression occurred at the highest dosage of 25 μg/mL, where TO_{SP}-3 reduced platelet aggregation to 86.82 %, reflecting a potent inhibitory capacity against ADP-mediated aggregation (Fig. 5, Table S3).

Platelet aggregation plays a crucial role in thrombus formation, wherein platelets adhere and aggregate to form stable clots, a process intricately regulated by various signaling molecules such as ADP. Upon binding to the P2Y12 receptors on the platelet surface, ADP activates intracellular pathways that induce calcium release, facilitating the activation of glycoprotein IIb/IIIa receptors, thereby promoting the aggregation and stabilization of platelet clots [70]. Previous studies have elucidated the role of sulfated polysaccharides, particularly fucoidans derived from *Laminaria japonica*, in mitigating platelet activation by substantially lowering aggregation [67]. Fucoidans exert this inhibitory effect by disrupting pathways triggered by agonists like thrombin and ADP, while also reducing von Willebrand factor (vWF) levels, which are essential for platelet binding. They can also bind to P-selectin, blocking platelet-fibrinogen interactions, and may inhibit GP IIb/IIIa receptors, thereby reducing stable aggregate formation [4]. Compared to aspirin, TO_{SP}-3 demonstrated a milder inhibition of platelet aggregation but showed a clear dose-dependent trend. While aspirin is a widely used antiplatelet agent, it is associated with gastrointestinal side effects and an increased risk of bleeding in long-term use [71]. In alignment with these mechanistic insights, the observed reduction in platelet aggregation with TO_{SP}-3 suggests that it effectively

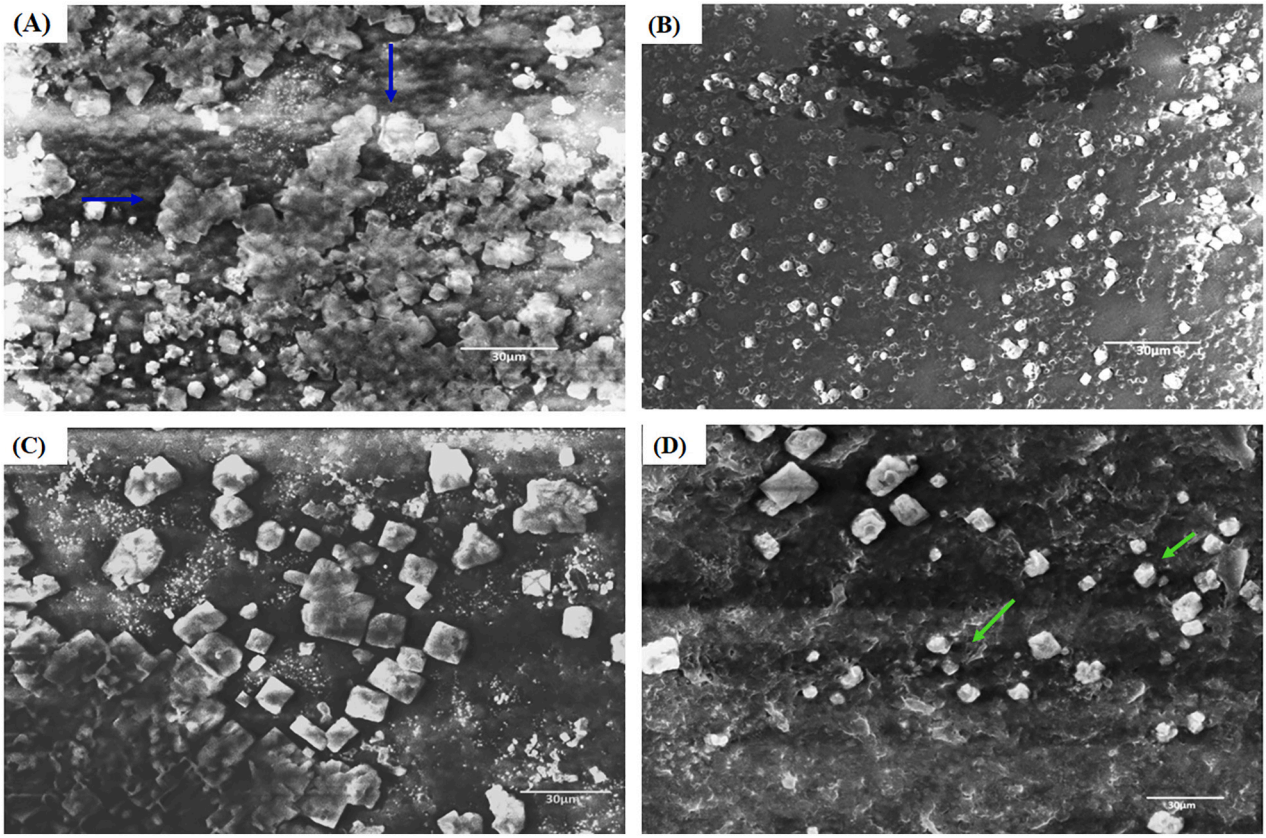

Fig. 5. Scanning electron micrographs (SEM) of platelet aggregation (scale bar = 30 μm). (A) Platelet aggregates induced by ADP (10 μM) as the aggregation agonist. (B) Platelet aggregates following treatment with aspirin (10 mM) as the positive control (antagonist). The blue arrow points to larger platelet aggregates. (C-D) Platelet aggregation in the presence of sulfated galactofucan (TO_{SP}-3 - 6.25 and 25 μg/mL). The green arrow indicates smaller, individual platelet aggregates.

inhibits platelet activation likely by interfering with key signaling pathways and molecules involved in platelet aggregation. This modulatory action on platelet activity highlights the significance of TO_{SP}-3 as a valuable therapeutic candidate, capable of preventing thrombus formation and managing clot-related disorders.

3.6.7. Possible structure-activity correlations of TO_{SP}-3

The physicochemical properties of TO_{SP}-3 and its desulfated hypothetical variant (TO_{SP}-3DS), including steric, electronic, and hydrophobic characteristics, were assessed utilizing ADME software (Table S4). TO_{SP}-3 showed significantly higher molecular polarizability (37.42) and topologically polarizable surface area (72.80) compared to its desulfated variant, TO_{SP}-3DS, with PI (28.70) and tPSA (69.30). These highlights the key role of sulfate moieties in enhancing the electronic properties of TO_{SP}-3 (Table S4). These properties of TO_{SP}-3 suggest an increased hydrophilicity and a greater binding affinity towards proteins, which can be corroborated to the hydrogen bonding interactions facilitated by the sulfate moieties. The minimal fluctuations in torsional energy, strain energy, rotational bond count, and molar refractivity associated with the sulfate group indicate its negligible influence on the binding affinity of TO_{SP}-3. In summary, the presence of sulfate moieties in TO_{SP}-3 significantly enhances its binding affinity and hydrophilicity, while also mitigating toxicity, making it a promising candidate for therapeutic applications [72,73]. Earlier literature supports that (1 → 3)-linked linear fucose residues, particularly those rich in 4-*O*-sulfated residues, have notable significance in enhancing the anticoagulant properties [59,60]. The polysaccharide TO_{SP}-3 is primarily composed of 4-*O*-sulfated α-fucose glycosyl moieties, intricately connected to 4-*O*-sulfated galactose units through (1 → 3) glycosidic bonds. The inherent negative charge of TO_{SP}-3, conferred by its sulfate groups, enhances its ability to form complexes with various coagulation proteins/enzymes, facilitating its anticoagulant properties [19]. Notably, Wang et al. (2019) reported that fucoidans with a high sulfate content and a low content of uronic acid (< 10 %) demonstrates remarkable anticoagulant activity [21]. Thus, the high sulfate content, specific sulfation pattern, and minimal uronic acid content in TO_{SP}-3 from *T. ornata* are likely key factors contributing to its potent anticoagulant efficacy.

4. Conclusions

This study highlights the significant anticoagulant effects of the sulfated galactofucan TO_{SP}-3, isolated from the brown seaweed *Turbinaria ornata*, highlighting its potential as a pharmacophore for thrombotic disorders through modulation of key components of the coagulation cascade. TO_{SP}-3 significantly prolongs aPTT by 3.79-fold and PT by 3.34-fold, indicating its impact on both intrinsic and extrinsic pathways, along with substantial downregulation of p-MARCKS and factor Xa expression by ~80 %. Further, TO_{SP}-3 significantly inhibits thrombin-catalyzed fibrin polymerization and intracellular calcium levels, along with ADP-induced platelet aggregation, highlighting its role in regulating key hemostatic processes. The anticoagulant activity of TO_{SP}-3 is primarily driven by its ability to interact with crucial coagulation factors, such as thrombin and Factor Xa, through electrostatic interactions facilitated by its high sulfate content. The distinct sulfate composition, patterns, and linkage structure of TO_{SP}-3 enable it to suppress FXa expression and inhibit thrombin-driven fibrin polymerization, resulting in a more efficient modulation of the coagulation cascade than heparin. These interactions disrupt fibrin formation, preventing excessive clotting while maintaining hemostatic balance. With its unique structural features, including α-(1 → 3) glycosidic linkages and approximately 18 % sulfation, particularly at the C-4 position, TO_{SP}-3 exhibits enhanced interactions with key coagulation proteins. Thus, TO_{SP}-3, emerges as a naturally derived, promising candidate for the development of effective and safer therapies for coagulation disorders.

CRediT authorship contribution statement

Ans Mariya George: Writing – review & editing, Writing – original draft, Visualization, Validation, Software, Methodology, Investigation, Formal analysis, Data curation. **Kajal Chakraborty:** Writing – review & editing, Writing – original draft, Validation, Supervision, Project administration, Investigation, Funding acquisition, Formal analysis, Conceptualization. **Silpa Kunnappilly Paulose:** Writing – review & editing, Visualization, Software, Formal analysis, Data curation. **Shifa Jalal:** Writing – review & editing, Visualization, Validation, Formal analysis. **Ashwin Ashok Pai:** Writing – review & editing, Methodology, Investigation, Formal analysis. **Shubhajit Dhara:** Writing – review & editing, Formal analysis, Data curation.

Ethical approval

This article does not report any studies involving animals or human participants conducted by the authors.

Declaration of competing interest

The authors declare that they have no known competing financial interests or personal relationships that could have appeared to influence the work reported in this paper.

Acknowledgements

The authors sincerely acknowledge the financial support provided by the Innovation in Science Pursuit for Inspired Research (INSPIRE) program of the Department of Science and Technology, New Delhi, India (Fellowship ID: IF220045). The authors express their sincere gratitude for the funding provided by the Indian Council of Agricultural Research (ICAR, New Delhi, India) for the Challenge Project (Grant No. Challenge/ICAR/216502; Project no: 1014515) and Department of Biotechnology (DBT) project "Development of polyketide and oligosaccharide analogues from economically important seaweeds as prospective angiotensin-converting inhibitors" (BT/PR40398/AAquote/3/995/2020). The authors extend their gratitude to the Director of ICAR-CMFRI and Dean, Faculty of Marine Sciences, Lakeside Campus, Cochin University of Science and Technology, for supporting the research activities. The authors express their gratitude to Stellixir Biotech Pvt Ltd for providing the cell line data required for the study. They are also grateful to SAIF, IIT Madras, and SCS, MG University, Kottayam, Kerala, India, for providing the spectroscopic data.

Appendix A. Supplementary data

Supplementary data to this article can be found online at https://doi.org/10.1016/j.ijbiomac.2025.141499.

Data availability

Data will be made available on request.

References

[1] A. Martins, C. Alves, J. Silva, S. Pinteus, H. Gaspar, R. Pedrosa, Sulfated polysaccharides from macroalgae-a simple roadmap for chemical characterization, Polymers 15 (2023) 399, https://doi.org/10.3390/polym15020399.
[2] E. Deniaud-Bouët, N. Kervarec, G. Michel, T. Tonon, B. Kloareg, C. Hervé, Chemical and enzymatic fractionation of cell walls from Fucales: insights into the structure of the extracellular matrix of brown algae, Ann. Bot. 114 (2014) 1203–1216, https://doi.org/10.1093/AOB/MCU096.
[3] J. Muthukumar, R. Chidambaram, S. Sukumaran, Sulfated polysaccharides and its commercial applications in food industries-a review, J. Food Sci. Technol. 58 (2021) 2453–2466, https://doi.org/10.1007/S13197-020-04837-0.
[4] G.S. Anisha, S. Padmakumari, A.K. Patel, A. Pandey, R.R. Singhania, Fucoidan from marine macroalgae: biological actions and applications in regenerative medicine,

drug delivery systems and food industry, Bioengineering 9 (2022) 472, https://doi.org/10.3390/bioengineering9090472.
[5] S. Luthuli, S. Wu, Y. Cheng, X. Zheng, M. Wu, H. Tong, Therapeutic effects of fucoidan: a review on recent studies, Mar. Drugs 17 (2019) 487, https://doi.org/10.3390/md17090487.
[6] J. Yu, Q. Li, J. Wu, X. Yang, S. Yang, W. Zhu, Y. Liu, W. Tang, S. Nie, A. Hassouna, W.L. White, Y. Zhao, J. Lu, Fucoidan extracted from sporophyll of *Undaria pinnatifida* Ggrown in Weihai, China – chemical composition and comparison of antioxidant activity of different molecular weight fractions, Front. Nutr. 8 (2021) 636930, https://doi.org/10.3389/fnut.2021.636930.
[7] N.M.A. Ponce, C.A. Pujol, E.B. Damonte, M.L. Flores, C.A. Stortz, Fucoidans from the brown seaweed *Adenocystis utricularis*: extraction methods, antiviral activity and structural studies, Carbohydr. Res. 338 (2003) 153–165, https://doi.org/10.1016/S0008-6215(02)00403-2.
[8] Y. Asada, A. Yamashita, Y. Sato, K. Hatakeyama, Pathophysiology of atherothrombosis: mechanisms of thrombus formation on disrupted atherosclerotic plaques, Pathol. Int. 70 (2020) 309, https://doi.org/10.1111/pin.12921.
[9] M. Manggau, M. Hamzah, S. Mamada, W.B. Nurdin, E.N. Zaenuddin, Anticoagulant activities of brown seaweed *Sargassum cristaefolium* extract, J. Phys. Conf. Ser. 1341 (2019) 072006, https://doi.org/10.1088/1742-6596/1341/7/072006.
[10] A.C. Nelson, M.A. Kelley, L.M. Haynes, K. Leiderman, Mathematical models of fibrin polymerization: past, present, and future, Curr. Opin. Biomed. Eng. 20 (2021) 100350, https://doi.org/10.1016/j.cobme.2021.100350.
[11] A. Lichota, E.M. Szewczyk, K. Gwozdzinski, Factors affecting the formation and treatment of thrombosis by natural and synthetic compounds, Int. J. Mol. Sci. 21 (2020) 7975, https://doi.org/10.3390/ijms21217975.
[12] S. Wei, A. Sawhney, H. Khandait, A. Meda, V. Gupta, R. Jain, An update on applications and limitations of direct oral anticoagulants, Egypt, J. Intern. Med. 35 (2023) 26, https://doi.org/10.1186/S43162-023-00212-5.
[13] S. Ballestri, E. Romagnoli, D. Arioli, V. Coluccio, A. Marrazzo, A. Athanasiou, M. Di Girolamo, C. Cappi, M. Marietta, M. Capitelli, Risk and management of bleeding complications with direct oral anticoagulants in patients with atrial fibrillation and venous thromboembolism: a narrative review, Adv. Ther. 40 (2023) 41–66, https://doi.org/10.1007/s12325-022-02333-9.
[14] M. Heestermans, G. Poenou, H. Hamzeh-Cognasse, F. Cognasse, L. Bertoletti, Anticoagulants: a short history, their mechanism of action, pharmacology, and indications, Cells 11 (2022) 3214, https://doi.org/10.3390/cells11203214.
[15] A. Adrien, A. Bonnet, D. Dufour, S. Baudouin, T. Maugard, N. Bridiau, Anticoagulant activity of sulfated ulvan isolated from the green macroalga *Ulva rigida*, Mar. Drugs 17 (2019) 291, https://doi.org/10.3390/md17050291.
[16] M.F. de Jesus Raposo, A.M. de Morais, R.M.S.C. de Morais, Marine polysaccharides from algae with potential biomedical applications, Mar. Drugs 13 (2015) 2967–3028, https://doi.org/10.3390/md13052967.
[17] F. Luan, J. Zou, Z. Rao, Y. Ji, Z. Lei, L. Peng, Y. Yang, X. He, N. Zeng, Polysaccharides from *Laminaria japonica*: an insight into the current research on structural features and biological properties, Food Funct. 12 (2021) 4254–4283, https://doi.org/10.1039/d1fo00311a.
[18] N. Shanthi, P. Arumugam, M. Murugan, M.P. Sudhakar, K. Arunkumar, Extraction of fucoidan from *Turbinaria decurrens* and the synthesis of fucoidan-coated AgNPs for anticoagulant application, ACS Omega 6 (2021) 30998–31008, https://doi.org/10.1021/acsomega.1c03776.
[19] Y. Yao, E.K.F. Yim, Fucoidan for cardiovascular application and the factors mediating its activities, Carbohydr. Polym. 270 (2021) 118347, https://doi.org/10.1016/j.carbpol.2021.118347.
[20] A.S. Silchenko, I.V. Taran, R.V. Usoltseva, N.V. Zvyagintsev, A.O. Zueva, N. K. Rubtsov, D.E. Lembikova, O.I. Nedashkovskaya, M.I. Kusaykin, M.P. Isaeva, S. P. Ermakova, The discovery of the fucoidan-active endo-1→4-α-L-fucanase of the GH168 family, which produces fucoidan derivatives with regular sulfation and anticoagulant activity, Int. J. Mol. Sci. 25 (2023) 218, https://doi.org/10.3390/ijms25010218.
[21] X. Wang, S. Wang, S. Huang, L. Zhang, Z. Ge, L. Sun, W. Zong, Purification of polyphenols from distiller's grains by macroporous resin and analysis of the polyphenolic components, Molecules 24 (2019) 1284, https://doi.org/10.3390/molecules24071284.
[22] X. Zhao, S. Dong, J. Wang, F. Li, A. Chen, B. Li, A comparative study of antithrombotic and antiplatelet activities of different fucoidans from *Laminaria japonica*, Thromb. Res. 129 (2012) 771–778, https://doi.org/10.1016/j.thromres.2011.07.041.
[23] M. Zubia, V. Stiger-Pouvreau, L. Mattio, C.E. Payri, H.L. Stewart, A comprehensive review of the brown macroalgal genus *Turbinaria* J.V. Lamouroux (Fucales, Sargassaceae), J. Appl. Phycol. 32 (2020) 2743–2760, https://doi.org/10.1007/s10811-020-02188-z.
[24] L. Qin, H. Xu, Y. He, C. Liang, K. Wang, J. Cao, C. Qu, J. Miao, Purification, chemical characterization and immunomodulatory activity of a sulfated polysaccharide from marine brown algae *Durvillaea antarctica*, Mar. Drugs 20 (2022) 223, https://doi.org/10.3390/MD20040223/S1.
[25] G. Surabhi, S. Dhara, A. Maneesh, K. Chakraborty, L. Valluru, S.R. Chenchula, Polygalacto-fucopyranose from marine alga as a prospective antihypertensive lead, Int. J. Biol. Macromol. 183 (2021) 589–599, https://doi.org/10.1016/J.IJBIOMAC.2021.04.140.
[26] S.S. Nielsen, Phenol-sulfuric acid method for total carbohydrates, in: S.S. Nielsen (Ed.), Food Analysis Laboratory Manual. Food Science Texts Series, Springer, Boston, MA, 2010, https://doi.org/10.1007/978-1-4419-1463-7_6.
[27] P. Kumar, V. Kumar, Estimation of uronic acids using diverse approaches and monosaccharide composition of alkali soluble polysaccharide from *Vitex negundo* Linn, Carbohydr. Polym. 165 (2017) 205–212, https://doi.org/10.1016/j.carbpol.2017.02.034.
[28] P.B. Torres, A. Nagai, C.E.P. Jara, J.P. Santos, F. Chow, D.Y.A.C. Dos Santos, Determination of sulfate in algal polysaccharide samples: a step-by-step protocol using microplate reader, Ocean Coast. Res. 69 (2021) e21021, https://doi.org/10.1590/2675-2824069.21-010pbt.
[29] K. Chakraborty, A. Maneesh, F. Makkar, Antioxidant activity of brown seaweeds, J. Aquat. Food Prod. Technol. 26 (2017) 406–419, https://doi.org/10.1080/10498850.2016.1201711.
[30] L. Qin, Y. Yang, W. Mao, Anticoagulant property of a sulfated polysaccharide with unique structural characteristics from the green alga *Chaetomorpha aerea*, Mar. Drugs 21 (2023) 88, https://doi.org/10.3390/MD21020088/S1.
[31] J.C. Stockert, R.W. Horobin, L.L. Colombo, A. Blázquez-Castro, Tetrazolium salts and formazan products in Cell Biology: viability assessment, fluorescence imaging, and labeling perspectives, Acta Histochem. 120 (2018) 159–167, https://doi.org/10.1016/j.acthis.2018.02.005.
[32] A.M. George, K. Chakraborty, S.K. Paulose, C. Bose, S. Dhara, Anti-coagulant effects of α-(1 → 3)/(1 → 4) linked sulfated galactofucan from brown macroalga *Sargassum plagiophyllum* (C. Agardh) in human umbilical vein endothelial cells, Food Biosci. 62 (2024) 105467, https://doi.org/10.1016/j.fbio.2024.105467.
[33] P.P. Bhuyan, R. Nayak, S. Patra, H.S. Abdulabbas, M. Jena, B. Pradhan, Seaweed-derived sulfated polysaccharides; the new age chemopreventives: a comprehensive review, Cancers 15 (2023) 715, https://doi.org/10.3390/cancers15030715.
[34] N.M. Liyanage, D.P. Nagahawatta, T.U. Jayawardena, K.K.A. Sanjeewa, H.H.A.C. K. Jayawrdhana, J.I. Kim, Y.J. Jeon, Sulfated polysaccharides from seaweeds: a promising strategy for combatting viral diseases—a review, Mar. Drugs 21 (2023) 461, https://doi.org/10.3390/md21090461.
[35] Y. Wang, M. Xing, Q. Cao, A. Ji, H. Liang, S. Song, Biological activities of fucoidan and the factors mediating its therapeutic effects: a review of recent studies, Mar. Drugs 17 (2019) 183, https://doi.org/10.3390/md1703018.
[36] S. Ermakova, R. Sokolova, S.M. Kim, B.H. Um, V. Isakov, T. Zvyagintseva, Fucoidans from brown seaweeds *Sargassum hornery*, *Eclonia cava*, *Costaria costata*: structural characteristics and anticancer activity, Appl. Biochem. Biotechnol. 164 (2011) 841–850, https://doi.org/10.1007/S12010-011-9178-2.
[37] T.T. Thanh, V.T. Tran, Y. Yuguchi, L.M. Bui, T.T. Nguyen, Structure of fucoidan from brown seaweed *Turbinaria ornata* as studied by electrospray ionization mass spectrometry (ESIMS) and small angle X-ray scattering (SAXS) techniques, Mar. Drugs 11 (2013) 2431–2443, https://doi.org/10.3390/md11072431.
[38] S. Lakshmana Senthil, T. Vinothkumar, D. Geetharamani, T. Marudhupandi, G. Suja, N.S. Sindhu, Fucoidan—a novel α-amylase inhibitor from *Turbinaria ornata* with relevance to NIDDM therapy, Biocatal. Agric. Biotechnol. 3 (2014) 66–70, https://doi.org/10.1016/j.bcab.2014.02.003.
[39] I.N. Taleb-Mokhtari, M. Rahal-Sekkal, G. Vergoten, Modified UBFF calculations of the α-l-fucopyranose molecule in the crystalline state, Spectrochim. Acta A Mol. Biomol. Spectrosc. 59 (2003) 607–616, https://doi.org/10.1016/S1386-1425(02)00211-1.
[40] X.G. Zhang, D.J. Siveter, D. Waloszek, A. Maas, An epipodite-bearing crown-group crustacean from the Lower Cambrian, Nature 449 (2007) 595–598, https://doi.org/10.1038/nature06138.
[41] Z. Zhang, F. Wang, X. Wang, X. Liu, Y. Hou, Q. Zhang, Extraction of the polysaccharides from five algae and their potential antioxidant activity in vitro, Carbohydr. Polym. 82 (2010) 118–121, https://doi.org/10.1016/j.carbpol.2010.04.031.
[42] K. Wang, X. Xu, Q. Wei, Q. Yang, J. Zhao, Y. Wang, X. Li, K. Ji, S. Song, Application of fucoidan as treatment for cardiovascular and cerebrovascular diseases, Ther. Adv. Chronic Dis. 13 (2022) 20406223221076891, https://doi.org/10.1177/20406223221076891.
[43] M.T. Ale, A.S. Meyer, Fucoidans from brown seaweeds: an update on structures, extraction techniques and use of enzymes as tools for structural elucidation, RSC Adv. 3 (2013) 8131–8141, https://doi.org/10.1039/c3ra23373a.
[44] A. Bettiol, S. Galora, F.R. Argento, E. Fini, G. Emmi, I. Mattioli, G. Bagni, C. Fiorillo, M. Becatti, Erythrocyte oxidative stress and thrombosis, Expert Rev. Mol. Med. 24 (2022) e31, https://doi.org/10.1017/erm.2022.25.
[45] M. Becatti, A. Mannucci, F.R. Argento, S. Gitto, F. Vizzutti, F. Marra, N. Taddei, C. Fiorillo, G. Laffi, Super-resolution microscopy reveals an altered fibrin network in cirrhosis: the key role of oxidative stress in fibrinogen structural modifications, Antioxidants 9 (2020) 737, https://doi.org/10.3390/antiox9080737.
[46] N.A. Mohd Fauziee, L.S. Chang, W.A. Wan Mustapha, A.R. Md Nor, S.J. Lim, Functional polysaccharides of fucoidan, laminaran and alginate from Malaysian brown seaweeds (*Sargassum polycystum*, *Turbinaria ornata* and *Padina boryana*), Int. J. Biol. Macromol. 167 (2021) 1135–1145, https://doi.org/10.1016/J.ijbiomac.2020.11.067.
[47] X.T. Ma, X.Y. Sun, K. Yu, B.S. Gui, Q. Gui, J.M. Ouyang, Effect of content of sulfate groups in seaweed polysaccharides on antioxidant activity and repair effect of subcellular organelles in injured HK-2 cells, Oxidative Med. Cell. Longev. 2017 (2017) 2542950, https://doi.org/10.1155/2017/2542950.
[48] S.H.S. Khalafu, W.M. Wan Aida, S.J. Lim, M.Y. Maskat, Effects of deodorisation methods on volatile compounds, chemical properties and antioxidant activities of fucoidan isolated from brown seaweed (*Sargassum* sp.), Algal Res. 25 (2017) 507–515, https://doi.org/10.1016/j.algal.2017.06.018.
[49] S. Sellimi, N. Kadri, V. Barragan-Montero, H. Laouer, M. Hajji, M. Nasri, Fucans from a Tunisian brown seaweed *Cystoseira barbata*: structural characteristics and antioxidant activity, Int. J. Biol. Macromol. 66 (2014) 281–288, https://doi.org/10.1016/j.ijbiomac.2014.02.041.
[50] C.M. Dore, M.G.das C. Faustino Alves, L.S. Will, T.G. Costa, D.A. Sabry, L.A. de Souza Rêgo, C.M. Accardo, H.A. Rocha, L.G. Filgueira, E.L. Leite, A sulfated

polysaccharide, fucans, isolated from brown algae *Sargassum vulgare* with anticoagulant, antithrombotic, antioxidant and anti-inflammatory effects, Carbohydr. Polym. 91 (2013) 467–475, https://doi.org/10.1016/j.carbpol.2012.07.075.
[51] M. Dhahri, *Cystoseira myrica*: from beach-cast seaweed to fucoidan with antioxidant and anticoagulant capacity, Front. Mar. Sci. 10 (2023) 1327408, https://doi.org/10.3389/fmars.2023.1327408.
[52] O.N. Pozharitskaya, E.D. Obluchinskaya, A.N. Shikov, Mechanisms of bioactivities of fucoidan from the brown seaweed *Fucus vesiculosus* L. of the Barents Sea, Mar. Drugs 18 (2020) 275, https://doi.org/10.3390/md18050275.
[53] Q. Chen, M. Zhang, Y. Liu, W. Liu, C. Peng, L. Zheng, Sulfated polysaccharides with anticoagulant potential: a review focusing on structure-activity relationship and action mechanism, Chem. Biodivers. 21 (2024) e202400152, https://doi.org/10.1002/cbdv.202400152.
[54] E.T. Goh, G. Kirby, R. Jayakumar, X.J. Liang, A. Tan, Accelerated wound healing using nanoparticles, in: M.R. Hamblin, P. Avci, T.W. Prow (Eds.), Nanoscience in Dermatology, Academic Press, New York, 2016, pp. 281–304, https://doi.org/10.1016/B978-0-12-802926-8.00023-9.
[55] O.M. Al-Amer, The role of thrombin in haemostasis, Blood Coagul. Fibrinolysis 33 (2022) 145–148, https://doi.org/10.1097/MBC.0000000000001130.
[56] M.R. Irhimeh, J.H. Fitton, R.M. Lowenthal, Pilot clinical study to evaluate the anticoagulant activity of fucoidan, Blood Coagul. Fibrinolysis 20 (2009) 607–610, https://doi.org/10.1097/MBC.0b013e32833135fe.
[57] M.B. Mansour, R. Balti, L. Yacoubi, V. Ollivier, F. Chaubet, R.M. Maaroufi, Primary structure and anticoagulant activity of fucoidan from the sea cucumber *Holothuria polii*, Int. J. Biol. Macromol. 121 (2019) 1145–1153, https://doi.org/10.1016/j.ijbiomac.2018.10.129.
[58] S. Shen, X. Chen, Z. Shen, H. Chen, Marine polysaccharides for wound dressings application: an overview, Pharmaceutics 13 (2021) 1666, https://doi.org/10.3390/pharmaceutics13101666.
[59] R.J. Fonseca, G.R. Santos, P.A. Mourão, Effects of polysaccharides enriched in 2,4-disulfated fucose units on coagulation, thrombosis and bleeding. Practical and conceptual implications, Thromb. Haemost. 102 (2009) 829–836, https://doi.org/10.1160/TH08-11-0773.
[60] N.E. Ustyuzhanina, N.A. Ushakova, M.E. Preobrazhenskaya, M.I. Bilan, E. A. Tsvetkova, V.B. Krylov, N.A. Anisimova, M.V. Kiselevskiy, N.V. Krukovskaya, C. Li, G. Yu, S. Saran, R.K. Saxena, A.I. Usov, N.E. Nifantiev, Fucoidans as a platform for new anticoagulant drugs discovery, Pure Appl. Chem. 86 (2014) 1365–1375, https://doi.org/10.1515/pac-2014-0404.
[61] M.S. Pereira, B. Mulloy, P.A.S. Mourão, Structure and anticoagulant activity of sulfated fucans. Comparison between the regular, repetitive, and linear fucans from echinoderms with the more heterogeneous and branched polymers from brown algae, J. Biol. Chem. 274 (1999) 7656–7667, https://doi.org/10.1074/JBC.274.12.7656.
[62] N.A. Ushakova, G.E. Morozevich, N.E. Ustyuzhanina, M.I. Bilan, A.I. Usov, N. E. Nifantiev, M.E. Preobrazhenskaya, Anticoagulant activity of fucoidans from brown algae, Biochem. Moscow Suppl. Ser. B 3 (2009) 77–83, https://doi.org/10.1134/S1990750809010119.
[63] K. Neubauer, B. Zieger, Endothelial cells and coagulation, Cell Tissue Res. 387 (2022) 391–398, https://doi.org/10.1007/s00441-021-03471-2.
[64] T. Nishino, A. Fukuda, T. Nagumo, M. Fujihara, E. Kaji, Inhibition of the generation of thrombin and factor xa by a fucoidan from the brown seaweed *Ecklonia kurome*, Thromb. Res. 96 (1999) 37–49, https://doi.org/10.1016/s0049-3848(99)00060-2.
[65] M.R. Buchanan, B. Boneu, F. Ofosu, J. Hirsh, The relative importance of thrombin inhibition and factor Xa inhibition to the antithrombotic effects of heparin, Blood 65 (1985) 198–201, https://doi.org/10.1182/blood.v65.1.198.198.
[66] A. Cumashi, N.A. Ushakova, M.E. Preobrazhenskaya, A. D'Incecco, A. Piccoli, L. Totani, N. Tinari, G.E. Morozevich, A.E. Berman, M.I. Bilan, A.I. Usov, N. E. Ustyuzhanina, A.A. Grachev, C.J. Sanderson, M. Kelly, G.A. Rabinovich, S. Iacobelli, N.E. Nifantiev, A comparative study of the anti-inflammatory, anticoagulant, antiangiogenic, and antiadhesive activities of nine different fucoidans from brown seaweeds, Glycobiology 17 (2007) 541–552, https://doi.org/10.1093/glycob/cwm014.
[67] A. Chen, F. Zhang, J. Shi, X. Zhao, M. Yan, Mechanism study of endothelial protection and inhibits platelet activation of low molecular weight fucoidan from *Laminaria japonica*, J. Ocean Univ. China 15 (2016) 918–922, https://doi.org/10.1007/s11802-016-3016-7/metrics.
[68] R.A. Risman, H.A. Belcher, R.K. Ramanujam, J.W. Weisel, N.E. Hudson, V. Tutwiler, Comprehensive analysis of the role of fibrinogen and thrombin in clot formation and structure for plasma and purified fibrinogen, Biomolecules 14 (2024) 230, https://doi.org/10.3390/biom14020230/s1.
[69] J.W. Weisel, R.I. Litvinov, Fibrin formation, structure and properties, Subcell. Biochem. 82 (2017) 405–456, https://doi.org/10.1007/978-3-319-49674-0_13.
[70] R.T. Dorsam, S.P. Kunapuli, Central role of the P2Y12 receptor in platelet activation, J. Clin. Invest. 113 (2004) 340–345, https://doi.org/10.1172/jci20986.
[71] E.S. Huang, L.L. Strate, W.W. Ho, S.S. Lee, A.T. Chan, Long term use of aspirin and the risk of gastrointestinal bleeding, Am. J. Med. 124 (2011) 426–433, https://doi.org/10.1016/j.amjmed.2010.12.022.
[72] W. Bououden, Y. Benguerba, Computational quantum chemical study, drug-likeness and in silico cytotoxicity evaluation of some steroidal anti-inflammatory drugs, J. Drug Deliv. Ther. 10 (2020) 68–74, https://doi.org/10.22270/jddt.v10i3-s.4165.
[73] A.R. Leach, V.J. Gillet, Molecular descriptors, in: An Introduction to Chemoinformatics, Springer, Dordrecht, 2007, pp. 53–74, https://doi.org/10.1007/978-1-4020-6291-9.